CALCITE RECRYSTALLIZATION AT EQUILIBRIUM AS INFLUENCED BY THE INITIAL ROWTH RATE AND PH

by

KAREN M. JUAREZ

A Dissertation submitted to the

Graduate School-Newark

Rutgers, The State University of New Jersey

in partial fulfillment of the requirements

for the degree of

Master of Science

Graduate Program in Environmental Geology

written under the direction of

Dr. Ashaki Rouff

and approved by

_____

_____

_____

Newark, New Jersey

May 2020

ABSTRACT OF THE DISSERTATION

Calcite Recrystallization at Equilibrium as Influenced by Initial Growth Rate and pH

By KAREN JUAREZ

Dissertation Director:

Ashaki Rouff

The mineral calcite was evaluated for recrystallization, a process known to change the location of ions in the mineral lattice without apparent change in mineral chemistry. Calcite lattice reconfiguration is cause for concern because it is a ubiquitous mineral with considerable reactivity that plays an important role in contaminant uptake and possible release. The intrinsic factor, crystal growth, and extrinsic factor, pH, were selected as possible driving forces for calcite recrystallization. Calcite growth experiments were conducted using a dual syringe pump technique. Geochemical analysis revealed calcite growth to be affected by syringe pump rate, a variable that showed no correlation with surface roughness. In order to trace recrystallization of laboratory grown calcite, an ion exchange technique with ^{45}Ca radioisotope and a separate ^{40}Ca stable isotope concentration analysis were used during resuspension batch experiments. There was no evident change in any of the radioisotope tracer experiments, indicating calcite stability. Additionally, ^{40}Ca stable isotope concentration measurements support the same idea of calcite stability and its ability to maintain dynamic equilibrium.

ACKNOWLEDGEMENTS

First, I would like to thank Rutgers University-Newark and the Department of Earth and Environmental Science. I would like to thank my advisor, Ashaki Rouff. Thank you for the opportunity to conduct geochemical research, I am grateful to have worked in your magnificent lab and been part of your team. I would also like to thank Evert Elzinga for guiding me in the radiation laboratory and Adam Kustka for allowing me work in your radio isotope laboratory. Additionally, I would like to thank my committee member Dimitrios Ntarlagiannis for taking the time to look at and review my work.

I also have to thank the geochemistry PhD graduate students for their support and help. I would like to thank Omanjana for helping me run the analytical instruments for concentration reading. I want to thank Alon for helping me with calcite imaging and having creative conversation about geochemical research. I would especially like to thank Marlon for assisting me with analytical instruments and always being there for me. I would like to thank Mike for helping me make some of the components of my reactor.

I would also like to thank my friends Stephanie, Amna, Erika, Ashley and Gracia. Thank you for your continued friendship over the years, for your love and support. I would also like to thank my family for being my forever support system and to my dog kiwi for being my companion. To my mom and dad, for inspiring me to go further and for loving me so kindly. To my brother and sister, Cesar and Gissel, for inspiring me in everything I do, for guiding me in difficult times and motivating me through anything. The completion of this thesis would not have been possible without your love and support.

TABLE OF CONTENTS

LIST OF TABLES

LIST OF FIGURES

Introduction

The mineral calcite has a chemical composition of $CaCO_3$ and a rhombohedron crystal structure, both properties play an important role in its reactivity and stability (Reeder., 1983). Thermodynamically, calcite is the most stable carbonate mineral under most environments, therefore it is least soluble, making it one of the most prevalent minerals on earth's surface (Eby., 2004). Calcite is an important mineral because it holds a record of water chemistry in specific environments and through time. Calcium carbonates, primarily calcite, are used for their ability to sorb inorganic environmental contaminants through the processes of crystallization and sorption (Aziz et al., 2007). Through previous analysis of contaminant uptake, it has been implied that recrystallization of calcite could be occurring. Recrystallization is a kinetic controlled process, driven by the rates of dissolution and precipitation. During recrystallization a mineral can undergo changes in isotopic composition and/or reconfiguration throughout the crystal lattice. Evidence of calcite reconfiguration is of concern because bulk mineral stability determines the mobility of contaminants sequestered by calcite.

Carbonate Chemistry

Calcite is comprised of two ions, calcium (Ca^{2+}) and carbonate (CO_3^{2-}); therefore, carbonate chemistry plays an important role in calcite chemistry. Carbonate chemistry begins in the atmosphere, where carbon dioxide (CO_2) dissolves in water (H_2O) to form carbonic acid (H_2CO_3):

$$H_2O_{(l)} + CO_{2(g)} = H_2CO_{3(aq)} \quad (1)$$

The equilibrium constant for this reaction is:

$$K_{CO2} = [H_2CO_3]/pCO_2 \quad (2)$$

The K_{CO2} value is Henry's gas constant, this value is temperature dependent. At 25°C, the value is $10^{-1.47}$, at 0°C it's $10^{-1.11}$, the solubility of CO_2 in a liquid therefore increases as temperature decreases. The pCO_2 value is the partial pressure of CO_2 in the atmosphere, the concentration expressed in units of ppm or bar, with current concentrations reaching values of ~400ppm. The H_2CO_3 value is the concentration of carbonic acid. The amount of carbonic acid is directly proportional to the concentration of CO_2 in the air (pCO_2), therefore as CO_2 in the atmosphere increases, so does H_2CO_3 concentration.

Once carbonic acid is formed it can dissociate to form the bicarbonate ion (HCO_3^-):

$$H_2CO_3 = H^+ + HCO_3^- \quad (3)$$

The equilibrium constant for this reaction is:

$$K_1 = [H^+]\,[HCO_3^-]/\,[H_2CO_3] \quad (4)$$

The K_1 at 25°C has a constant value of $10^{-6.35}$. Since carbonic acid is a weak acid that only partially dissociates, it has a low K value. This equation can also be rewritten in terms of H^+ to determine the pH of water in equilibrium with carbon dioxide. Depending on temperature, if the value of K_1 is lower, it dissociates less, and the result is a less acidic solution. As temperature increases, pH increases and carbon dioxide decreases.

$$pH = -\log[H^+] \quad (5)$$

The bicarbonate ion (HCO_3^-) is likely to lose a hydrogen ion to form the aqueous carbonate ion:

$$HCO_3^- = H^+ + CO_3^{2-} \quad (6)$$

The equilibrium constant for this reaction is:

$$K_2 = [H^+]\,[CO_3^{2-}]/\,[HCO_3^-] \quad (7)$$

The K_2 at 25°C has a value of $10^{-10.33}$. When $[H_2CO_3] = [HCO_3^-]$, pH= 6.35, and when $[HCO_3^-] = [CO_3^{2-}]$, pH=10.33 (Fig.1). When pH<6.35, H_2CO_3 predominates because high concentrations of H^+ drive the system to produce more carbonic acid from bicarbonate ($HCO_3^- + H^+ = H_2CO_3$). When 6.35<pH<10.33, HCO_3^- is the dominant species in solution. When pH<10.33, CO_3^{2-} dominates because bicarbonate will release H^+ to neutralize OH^- producing carbonate anion and water ($HCO_3^- + OH^- = CO_3^{2-} + H_2O$).

$$H_2O = H^+ + OH^- \quad (8)$$

$$K_w = [H^+]\,[OH^-] \quad (9)$$

Calcite Chemistry

Calcium carbonate occurs as the three mineral forms: calcite, vaterite, aragonite. At earth's surface calcite is the most thermodynamically stable and most abundant of the three forms, it is the least soluble due to its chemical makeup and morphology (Plummer and Busenberg., 1982). Calcite has an abundance as high as 20% in carbonate minerals, up to 30% of $CaCO_3$ is buried in sediment, while the rest is present as dissolved species. Additionally, the chemistry of aquifers or soils with only 1% calcite will be carbonate

dominant due to dissolution (Tang et al., 2019; Feely et al.,2004; Ryan., 2014). Therefore, the surrounding environmental conditions have a great effect on calcite solubility.

Many surface and groundwaters are saturated with calcite, the reactions that control its distribution in the environment are precipitation and dissolution. The kinetics of carbonate mineral dissolution and precipitation reactions in comparison to other minerals is “moderate”, being faster than clay minerals, yet slower than for typical evaporite minerals (Reeder., 1983). Calcite can either precipitate or dissolve depending on external conditions, which will be discussed after the chemical reactions.

The first reference point in calcite chemical kinetics is equilibrium. Equilibrium between a solid and an aqueous solution is when the forward dissolution and reverse precipitation reaction rates are equal so that no net change occurs, the reaction that describes this process is:

$$CaCO_3 = Ca^{2+} + CO_3^{2-} \quad (10)$$

The equilibrium constant for this reaction is the solubility product:

$$K_{sp} = [Ca^{2+}]\,[\,CO_3^{2-}] \quad (11)$$

The forward dissolution reaction for calcite can be written several ways (Plummer et al., 1978; Eby., 2004; Brantley et al., 2008). The principle dissolution equilibrium reaction is one that occurs under natural environmental conditions. Naturally water and carbon dioxide yield carbonic acid:

$$H_2O + CO_{2(g)} = H_2CO_3 \quad (1)$$

Carbonic acid in water dissolves carbonates, the dissolution reaction of calcite is thus:

$$CaCO_3 + H_2O + CO_2 = Ca^{2+} + 2HCO_3^- \quad (12)$$

The equilibrium constant for this reaction is:

$$K_{eq}=[Ca^{2+}]\,[HCO_3^-]^2/\,pCO_2 = 10^{-8.41} \quad (13)$$

Or also represented as:

$$CaCO_3 + H_2CO_3 = Ca^{2+} + 2HCO_3^- \quad (14)$$

Between pH 6.4 – 10.33 $2HCO_3^-$ is the dominant species, therefore the first equation is typically used for calculations. Depending on pH other acids will dissolve calcite.

In conditions with low acid concentrations, the following reaction occurs:

$$CaCO_3 + H^+ = Ca^{2+} + HCO_3^- \quad (15)$$

In conditions with strong acid concentrations:

$$CaCO_3 + 2H^+ = Ca^{2+} + H_2O + CO_2 \quad (16)$$

Carbonates are even soluble in waters devoid of CO_2:

$$CaCO_3 + H_2O = Ca^{2+} + HCO_3^- + OH^- \quad (17)$$

The precipitation reactions for calcite involves the same reactions as dissolution but in reverse. The waters where carbonates grow are between pH 6.4 – 10.33, bicarbonate is the most abundant:

$$Ca^{2+} + HCO_3^- = CaCO_3 + H^+ \quad (15)$$

High enough calcium and bicarbonate will form the mineral:

$Ca^{2+} + 2HCO_3^- = CaCO_3 + H_2O + CO_2$ (12)

If a base is added:

$Ca^{2+} + HCO_3^- + OH^- = CaCO_3 + H_2O$ (17)

Variables That Affect Calcite Solubility

Whether calcite's reaction moves in the direction of the forward dissolution reaction, or in the reverse precipitation reaction depends on conditions such as pH, pressure, and temperature. These three variables are often interrelated. It is clear that the solubility of calcite is dependent on the partial pressure of $CO_{2(g)}$ above solution. According to Henry's law, an increase in atmospheric $CO_{2(g)}$ will result in an increase in aqueous $CO_{2\,(aq)}$ concentration (1). If calcite dissolution is considered in terms of Le Chatelier's principle, which indicates that increasing the concentration of any of the products will shift the equilibrium in the direction of the reactants (12), there will be more dissolved calcium and bicarbonate as a result of calcite dissolution. Although carbonic acid is not a strong acid, its dissociation will decrease the system pH and cause a decrease mineral stability. If there was a decrease in CO_2 calcite dissolution would decrease and calcite precipitation increase.

Calcite stability decreases as temperature increases. The reason for this is because of the effect increasing temperature has on dissolved CO_2 in water. An increase in water temperature causes a decrease in CO_2 concentration ($CO_{2(g)}$ is less soluble in hot water than in cold water), therefore there is less carbonic acid and as a result an increase in calcite precipitation.

Calcite solubility is also strongly dependent on metal ions in aqueous solution. For example, the presence of Mg^{2+} inhibits calcite growth (Berner., 1975), alters dissolution kinetics (Alkattan et al., 2002), and influences surface morphology (Davis et al., 2004). Another factor that effects calcite solubility is organic activity. Organisms aid in the precipitation of calcium carbonate indirectly by removing CO_2 from water in the process of photosynthesis (Liang et al., 2018). While it is clear that extrinsic factors, such as the aforementioned have important controls on calcite solubility, it should be noted that intrinsic factors, such as mineral structure and morphology also promote calcite solubility (Lasaga and Blum., 1986).

Calcite Recrystallization

Calcite is considered a thermodynamically stable mineral because it is the least soluble calcium carbonate mineral (Langmuir., 1997), however there is not enough kinetic data available to determine its equilibrium stability in geochemical environments. In previous years calcite kinetic studies heavily involved sorption analysis. The potential of calcite to sequester trace elements has been studied extensively (Zachara et al., 1991; Stipp et al.,1998; Reeder et al., 2004; Rouff et al., 2005; Elzinga et al., 2006; Heberling et al., 2008; Ahmed et al., 2009). The reactions that can occur between a trace element and calcite include adsorption (surface bond between element and mineral), coprecipitation (element incorporated into bulk of mineral lattice) and surface precipitation (precipitation of a second mineral upon surface of initial mineral) (Fig.2). Sorption experiments have evidence that suggests mineral composition can be altered by replacement of $Ca^{2+}$from the surface of calcite. For example, results from Elzinga et al (2006) demonstrate divalent

metals, Zn^{2+}, Pb^{2+}, Cu^{2+}form inner-sphere adsorption complexes with the surface of calcite during extended reaction periods (2.5 yr.). Additionally, actinide elements (Neptunium (V)) present in nuclear wastes have also been found to replace calcium lattice sites (Heberling et al., 2008).

Results from sorption experiments have led to further inquiries about the stability of the calcite mineral lattice, weather it is susceptible to recrystallization, and what are the driving forces for recrystallization. Recrystallization involves the exchange of atoms bound to the mineral with atoms in solution, for calcite the concern is the ability for structural Ca^{2+} to exchange with dissolved Ca^{2+}(Fig.3). This type of ion exchange reaction can occur under equilibrated conditions where pressure, temperature and solution chemistry do not change, making it difficult to study the mechanism. Studying calcite recrystallization kinetics in a laboratory setting can help to further understand processes going on in applied settings, where calcite is used as a buffer or as treatment for wastewaters (Cravotta III and Trahan., 1999; Aziz et al., 2008; Jacob et al., 2018).

One of the first observations of calcite recrystallization was made by Mozeto et al. (1984), the study's goal was to determine the influence of calcite recrystallization on carbon isotope composition. Based on their conclusion they observed two-stage kinetics upon recrystallization. The first stage is described to be rapid and reaches steady state within the first hours of the experiment, the second stage is slower and does not reach steady state during the duration of a month or longer (Inks and Hahn, 1963; Reddy and Nancollas, 1971; Moller and Sastri, 1973; Mozeto et al.,1984; Davis et al., 1987; Zachara et al., 1991; Terte et al., 2010, 2012; Avrahamov et al., 2013). It is suggested that the initial rapid isotopic exchange can be attributed to exchange between surface atoms and

dissolved ions which is a common process that occurs at equilibrium (Groski and Fantle., 2016). The process that occurs during the slower, time dependent stage is still poorly understood. Davis et al. (1987) proposes that long- term ^{45}Ca exchange could be due to Ca^{2+} lattice penetration between underlying hydrated layers of the calcite surface. Zachara et al. (1991) and Larsen et al. (2010) suggest that lattice penetration is unlikely to exceed two mono layers in depth. A study by Tertre et al. (2010) describes the second stage with slower kinetics as quasi irreversible and suggests ^{45}Ca is deeply trapped in the mineral. Results that point to a direct indication of a driving force for recrystallization have yet to be determined.

Objectives and Hypothesis

Although evidence of recrystallization has been widely recognized, there is still insufficient kinetic data that provides definitive interpretations on calcite stability or on recrystallization reaction mechanism. The biggest challenge in mineral recrystallization research is the limitation of quantitative analysis by the availability of high-resolution instruments that provide information about the physical and chemical role of the crystal surface and bulk lattice. Nonetheless, the reasons to continue this search are significant. Recrystallization kinetics are typically examined by using radioactive isotope tracers, this methodology is advantageous in that isotopic exchange occurs between structural and dissolved ions without changing mineral properties (Groski and Fantle., 2016). The disadvantage to using radioactive isotopes is that their toxicities make microscopic imaging difficult for tracking crystallographic changes.

The purpose of this research is to add to the understanding of calcite recrystallization kinetics. The only previous analysis that indicates a driving force for recrystallization was conducted by Heberling et al (2016); therefore, this study aims to contribute kinetic analysis of intrinsic variables, those that are chemical such as mineral structure, and extrinsic variables, those that are physical such as pH, that could potentially drive calcite out of equilibrium. The following questions will be addressed: (1) Are there stages to reaching equilibrium? (2) What is the extent of calcite recrystallization, is it limited to the surface or is there also bulk lattice exchange? (3) Do intrinsic or extrinsic variables affect calcite recrystallization?

The research in this thesis focuses on the behavior of calcite in systems in which the mineral is considered stable. The potential for mineral restructuring under equilibrium conditions was evaluated by quantifying the release and/or exchange of structural Ca^{2+} with solution. I hypothesize that the calcite internal structure has the potential to exchange ions with solution based on the intrinsic variable of crystallinity and crystal growth rate. To explore this hypothesis, the first variable characterizes differences in crystallinity based on the amount of time calcite was allowed to grow and how those differences affect rates of exchange. This is accomplished by constructing a well-controlled growth environment, using the seeded constant addition technique discussed in detail in the materials and methods section. After calcite growth was characterized, mineral recrystallization was examined by using radioactive isotope ^{45}Ca exchange techniques in batch form to measure rates of exchange. Using Scanning Electron Microscopy (SEM) data to measure crystallographic differences due to crystal growth combined with ^{45}Ca exchange rates to quantify extent of recrystallization will help to

further understand the mechanisms that occur on a molecular scale during calcite recrystallization.

The second variable, pH, is extrinsic. Both pH 7.5 and pH 8.3 were selected because they have significant implications for environmental settings. As previously mentioned calcite is saturated at pH of 8.3, commonly found in most surface water environments. However, in systems where pH is found to be near 7.5, calcite is still able to precipitate and is relevant to waters with higher levels of carbonic acid present (e.g. ocean surface waters) (Langmuir.,1997; Bozlee., 2008; Land et al., 2015). A previous study by Rouff et al (2005) demonstrated the effect of different pH values on calcite sorbent properties. At equilibrium conditions calcite adsorbed Pb^{2+} at pH 8.2, at pH 7.3 and 9.4 calcite adsorbed and coprecipitated the metal and showed irreversibility. With evidence that suggests the influence of pH on sorption mechanisms, this current experiment explores the similar effect of pH but with exchange of the Ca^{2+} alkaline earth metal ion that leads to differences in rates, known as recrystallization. To date, there have been no studies that describe how differences in pH solution are involved in rates of recrystallization. The hypothesis for this thesis is that at pH 8.4, where calcite is saturated and under equilibrium, recrystallization is not expected. At pH 7.3, where more acidic conditions are prevalent, recrystallization might occur.

Methods

Calcite Experimental Set Up

The seeded constant addition method (Zhong et al., 1993; Tesoriero et al., 1996) was used to grow calcite through precipitation at different rates. At atmospheric $CO_{2(g)}$ pressure ($10^{-3.39}$ bar) the saturation pH of calcite is 8.3 (Langmuir., 1997). The ideal conditions for growing calcite require an open carbonate system where $CO_{2(g)}$ pressure is constant and the system is supersaturated with respect to calcite (Plummer and Busenberg., 1982). Calcite undergoes an exothermic reaction (releases heat energy, enthalpy $\Delta H < 0$) when there is a decrease in temperature, meaning dissolution occurs, consequently a rise in temperature will cause calcite to precipitate (Eby., 2004). Research relevant to calcite recrystallization is done at temperature equal to 25º C to prevent phase change and disequilibration.

All chemicals used for the growth experiments were reagent grade obtained from Fisher Scientific and all experiments were done in duplicate. The initial growth solution was prepared by dissolving 0.1M $NaNO_3$ in 1L Milli-Q water (18.0 MΩcm, < 2ppb dissolved organic carbon), additionally with 1mM $Ca(NO_3)_2{\cdot}4H_2O$ and 1mM $NaHCO_3$ in order to provide optimal ionization background for equilibrium, as was calculated using V.MINTEQ 3.1 (https://www.kth.se/). The initial growth solution was introduced to a 2000 mL KIMAX beaker reaction vessel that was mounted on top of an electric stir plate. The reaction vessels were covered with Lucite lids with holes for insertion of a pH meter or insertion of a pipette for sampling solution, for a gas dispersion tube, and for two

Nalgene tubes (5/16 ID) that deliver reaction solutions. The addition of 500 mg of calcite seed adjusted the initial growth solution to the desired steady state slight oversaturation at which calcite growth could begin. To achieve constant solution composition, growth experiments were performed at ambient room temperature and PCO_2 ($10^{-3.39}$ atm) was continuously bubbled to the growth solution via a PYREX fritted gas dispersion tube connected to an air pump (Fig.4). All solutions maintained a constant stir rate of 250 rpm with the use of a Nalgene floating stir bar in order to prevent the grinding of $CaCO_3$ crystals in the bottom of the vessel. The initial growth solution stabilized rapidly, within 2 days, at a pH value of about 8.3 before commencing crystal growth.

Before and during each experiment, the pH of the reacting solution was measured to determine growth stabilization in the supersaturated solution. Once pH reaches 8.3±1 equilibrium is reached. A Thermo-Scientific Orion 3 Star glass electrode was used to measure pH. Prior to pH measurement, the glass electrode was calibrated with Thermo Scientific buffer solutions 4.01, 7 and 10.1. In each experiment the addition of 0.1M Na_2CO_3 and 0.1M $Ca(NO_3)_2 \cdot 4H_2O$ caused a sharp increase in pH as a result of becoming more oversaturated with respect to calcite. By the end of each experiment, pH reached equilibrium value of 8.4±1.

Calcite Growth

$CaCO_3$ growth was induced by pumping in two solutions 0.1M Na_2CO_3 and 0.1M $Ca(NO_3)_2 \cdot 4H_2O$ in gas tight syringes (60 mL B-D) using a dual syringe pump (Harvard Apparatus-22). The volume of the reactant solutions used was 120 mL each. The

predetermined pump rates for growth reactions were 120 µL/min, 60 µL/min, and 30 µL/min. Crystal growth was carried out until each syringe volume completely reacted. At selected time intervals 10 mL aliquots of solution were sampled from the vessel using a 10mL syringe and separated from the solid crystal using a 0.45µm Whatman syringe filter. Immediately after the syringe pump stopped, the reaction solution was filtered through a 0.45 µm Millipore filter. The grown $CaCO_3$ was air dried for at least one week prior to further analysis. The amount of growth in all experiments was approximately 50 % of the initial seed weight.

^{40}Ca Calcite Resuspension

Two out of the three rates in which calcite was grown were selected for resuspension. Syringe pump rates of 120 µL/min and 60 µL/min were selected for further experimentation because at the fastest and intermediate growth rate, calcites surface would have developed surface roughness and surface energy that could potentially drive recrystallization. Calcite from each rate was introduced to pre-equilibrated solutions of pH 8.3 and pH 7.5. The composition of the pre-equilibrated solution was calculated using Phreeqc 3.1.7 (Table.1and 2). Respective concentrations of Ca $(NO_3)_2$ and NaHCO3 were added to 2L of Milli-Q water with 2g of reagent grade calcite, a continuous PCO_2 bubbling under a 250-rpm stir was maintained, a set up similar to the one used for calcite synthesis. For pH 8.3 a concentration of 0.826 mM Ca $(NO_3)_2$ and 1.6 mM $NaHCO_3$ was needed to bring the solution to equilibrium. The ionic strength conditions for pH 7.5 required were 36.4 mM Ca $(NO_3)_2$ and 0.325 mM $NaHCO_3$. To bring the solution to pH 7.5 a small amount of 72.45 mM HNO_3 was added to the solution. pH measurements

were conducted to confirm that equilibrium was reached. Both solutions were allowed to equilibrate for two weeks. The equilibrated solution was then separated from solid through a 0.45 µm Millipore filter.

Mineral resuspensions for calcite generated at pump rates 120 µL/min and 60 µL/min, each in pH 8.3 and pH 7.5 solutions, were done in duplicate. A 1:1 ratio between solution and mineral is necessary for equilibrium of the resuspended mineral. Therefore, a concentration of $8.2x10^{-4}$ M Ca^{2+} was present in both mineral and solution of pH 8.3 and $3.7x10^{-2}$ M Ca^{2+} was present for calcite and solution of pH 7.5. Each sample was prepared with 100 mL of the corresponding equilibrated solution. Blanks without any calcite were also included. First, 20.65 mg ($8.2x10^{-4}$ M) of calcite was introduced to 250 mL of pre-equilibrated pH 8.3 calcite solution in a 250 mL Nalgene wide mouth HDPE centrifuge bottle. Then, 100 mL of the resuspended calcite was separated using an Eppendorf adjustable volume pipette into a 125 mL HDPE bottle. For pH 7.5, an initial 200 mL solution was prepared instead due to limited amount of grown calcite. The amount of calcite used for pH 7.5 resuspension was 728 mg ($3.7x10^{-2}$ M). From the 200mL solution, 100 mL was separated by pipette into a 125 mL HDPE bottle. The exact procedure was followed for calcite grown at 120 µL/min and 60 µL/min rates.

The resuspension experiments were allowed to react for 106 days with sampling of aqueous solution done every week and then every other week. Samples were filtered and refrigerated for later analysis of total Ca by inductively coupled plasma optical emission spectroscopy (ICP-OES) using an Agilent Technologies 5110 SVDV instrument.

During calcite resuspension in the pre-equilibrated solution, pH measurements were also taken. After one month of calcite re-equilibration, pH measurements were taken every two weeks for the duration of the experiment. This was done for all experiments at pH 8.3 and 7.5.

^{45}Ca Calcite Resuspension

For resuspension experiments using ^{45}Ca as the radiotracer, a similar procedure as previously described for ^{40}Ca calcite resuspension was used. A 100 mL volume of pre-equilibrated calcite solution for each pH was separated by pipette into an HDPE bottle, and corresponding amounts of calcite were introduced to solution. The experiment was transferred to the radiotracer laboratory, where each solution was spiked with 400 Bq/mL of ^{45}Ca prepared from a diluted secondary stock solution. The blanks, which did not have any calcite, were also spiked with the same amount of ^{45}Ca. The experiments were sampled one hour before the time sampling of the ^{40}Ca resuspension experiments. Prior to sampling, each bottle was agitated to ensure homogenization of the sample solution. For each sampling, a 1.5 mL aliquot of aqueous solution was separated via pipette and filtered into a 2.0 mL microcentrifuge tube. The ^{45}Ca calcite resuspension experiments were allowed to react for the same amount of time of 106 days (Fig.5). Each sample was refrigerated until ^{45}Ca activity was ready to be measured by liquid scintillation counting. The pH was not measured for these experiments.

Morphology of $CaCO_3$

The $CaCO_3$ crystals grown at syringe pump rates of 120, 60, and 30 µL/min were measured by X-ray diffraction (XRD) using a BRUKER D8 Advance diffractometer with CuKα radiation at 20 kV and 5mA. Once all samples had air dried for approximately three weeks, they were lightly ground with a mortar and pestle and then tightly packed into individual specimen rings which are mounted on the instrument sample holder. The diffraction pattern was collected at a scanning rate of 0.02 degrees per second over the range of 20-70º 2θ. Scanning Electron Microscopy (SEM HITACHI S-4800) was used to examine the surface of calcite crystals grown at the different pump rates. The calcite crystals were coated with 3 nm iridium using the sputter coater (CRESINGTON 208 HR) to minimize the charge reflected on the images.

Total Ca Concentration

Total content of calcium in the ^{40}Ca experimental set up, including both growth and resuspension, was measured by ICP-OES. For calcite resuspension experiments at pH 8.3 a 1 mL aliquot of solution from the growth vessel was used for analysis, as well as a 1 mL aliquot from the resuspended solution. Each sample was diluted 1:10 by adding 1 mL aqueous sample to 9 mL of 2% HNO_3 in a test tube. Next, standards ranging from 1-10 ppm were prepared from a 1000 ppm Ca stock solution in a 50mL Falcon centrifuge tube that contained 0.01 M $NaNO_3$ in 2% HNO_3 background to match the matrix of the sample. A blank of 0.01 M $NaNO_3$ in 2% HNO_3 background, six standard solutions and all samples were placed in the autosampler holders. The ICP conditions selected to run

the analysis include, running triplicate analysis on each sample, selecting three Ca wavelengths: 393.366 nm, 396.847 nm, 422.673 nm, and measuring in synchronous vertical dual view (SVDV) mode. This same procedure was performed on calcite resuspension samples from pH 7.5 solutions, with the exception of diluting by a factor of 1:1,000 instead of 1:10.

^{45}Ca Measurements

The samples from the ^{45}Ca calcite resuspension solution were analyzed for the concentration of ^{45}Ca remaining in solution after exchange with bulk calcite. A 1.0 mL aliquot of the aqueous sample was mixed with 5.0 mL Ecoscint A, National Diagnostics scintillation cocktail and counted by liquid scintillation on a Coulter Beckman LS 6500 instrument for a counting time of 5 min.

Results

Calcite Precipitation Rates

Table 3. summarizes the properties of calcite grown at three different syringe pump rates. It should be noted that for samples taken at slower syringe pump rates, more volume is required and the precipitation time is longer, therefore there are more sampling time points. The growth period for calcite grown at syringe pump rates of 120 µL/min, 60 µL/min, and 30 µL/min are 17 h, 33h, and 65h, respectively. For all three growth solutions, equilibration is reached by the end of each experiment as indicated by reaching a pH of 8.4 ± 2. Considering constant pH during precipitation, calcite precipitation rates were determined using the following equation:

$$R = [Ca_{tot} - Ca_{aq}] \cdot r \quad (18)$$

where r represents the syringe pump rate, Ca_{aq} the remaining calcium in solution and Ca_{tot} the total concentration of calcium based on initial seed mass and Ca syringe concentration (0.013M $Ca(NO_3)_2$ + 0.005M $CaCO_{3(s)}$ = 0.018M). Calcite precipitation rates are expressed in logarithm form in Table 1. Calcite 120 at 120 µL/min, the fastest syringe pump rate has a precipitation rate of $10^{-5.67}$ mol s-1, calcite 60, 60 µL/min with $10^{-5.97}$ mol s^{-1}, calcite 30 with the slowest syringe pump rate 30 µL/min has a rate of $10^{-6.27}$ mol s^{-1}. Slower syringe pump rates give lower precipitation values.

The total aqueous concentration of Ca for each calcite growth experiment and its duplicate are summarized in Table 4. Ca concentrations for all systems increased with time. For calcite 120, 60and 30, Ca concentrations reached an average value of 6.04 - 8.3

ppm by the end of the experiment. Figure 6 shows how the concentration of Ca changes with time. In precipitation reactions, concentration of reactants over time decreases as they are being consumed and the reaction slows down. Since calcite was precipitated using the constant addition method, the reaction does not slow down and the reactants increase over time as they were not fully consumed. As a result, there is an excess of Ca in the vessel that is not yet precipitated. The calcite sample 120 in Figure 6 shows a sharp decline in concentration, however this does not mean there was no crystal growth. Such occurrence can be attributed to sampling error since there is evidence of crystal growth by the 50% increase in initial seeded material and the surface imaging described further in the next sections.

Calcium Carbonate Mineralogy

To confirm that the calcium carbonate precipitates were calcite XRD data was collected. The XRD patterns of all calcium carbonate precipitates are in Fig. 7. Only characteristic peaks that are found in calcite are shown, indicating no difference from the seeded material and confirming the formation of calcite in all samples. The patterns contain a characteristic calcite peak at $2\theta = 29.4^{\circ}$, it is the strongest diffraction peak and corresponds to the {104} surface (Ibrahim et al.,2012; Gao et al., 2017). Calcite can form scalenohedrons, rhombohedrons or hexagonal prisms. The {104} rhombohedron crystal face is the most stable out of the other common calcite crystal surfaces ({110}, {100}, {001}, {018}, {214}, {012}), having the lowest specific surface energy, being non-polar and cleaving perfectly along the {104} plane (Aquilano et al., 2000; Massaro et al., 2008; Heberling et al., 2014; Mavromatis et al., 2017). Calcite {104} is the expected

calcium carbonate polymorph of precipitated calcite 120, 60 and 30, as they have the same solution composition and because the {104} plane dominates in morphology for crystals obtained in the laboratory (Massaro et al., 2007). The other possible polymorphs of calcium carbonate include aragonite $2\theta = 25^{o}$ and vaterite $2\theta = 45.9^{o}$, for which no characteristic peaks were identified in the XRD patterns of the precipitated samples. With calcite being the most thermodynamically stable polymorph and its presence confirmed by diffraction peaks of the {104} plane, all samples were confirmed to be favorable for further experimentation.

Calcite Surface Imaging

Bulk analysis identification provided by XRD is combined with scanning electron microscopy for surface imaging to describe the extent of calcite precipitation. SEM images of the initial calcite seed and the calcite recovered from precipitation experiments are shown in Fig.8. Examination of the solids recovered from the vessel after the experiments suggests that crystal aggregation occurred during the experiments. The mechanistic aspect of the growth process has been extensively discussed and it is accepted that the growth and dissolution of calcite are controlled by surface reactions (Plummer et al., 1978; Reddy et al., 1981). At low supersaturation near equilibrium <0.2, growth proceeds by step flow, through the attachment of growth units to kink sites in steps (Teng et al., 2000; Cubillas and Anderson., 2010). A new step forms by the nucleation of an individual monolayer at the crystal surface, the advancement of mineral growth is aided by surface defects, including step dislocations. It is not the purpose of this study to go into detail on this subject, although observations of growth are typically

analyzed through Atomic Force Microscopy (AFM). The primary aim of this study is to look for a correlation, qualitatively, between the relative amount of surface roughness and the speed at which calcite was grown. Furthermore, the SEM images show that the surface roughness increased notably during crystal growth as the syringe pump rate increased. The comparison between calcite 120 at syringe pump rate of 120 µL/min, calcite 60, 60 µL/min and calcite at 30 µL/min and their duplicates is presented in Figures 8b, 8c and 8d. Calcite 120, precipitated with the shortest duration of time (17h), we begin to see aggregation in the form of layers being added to the surface. In the calcite 120 duplicate a different aggregation characteristic was observed, where the surface is agglomerated with smooth edges compared to the rest of the precipitates. Calcite 60 and 30 show an increase in individual layers. SEM observations did not reveal any difference in morphology from the seeded material (Fig 8a), all recovered calcite crystals exhibit the rhombohedral structure. The most appropriate selection for calcite resuspension is one that provides the least amount of possible driving force for recrystallization. Having precipitated calcite crystals in their most stable form at equilibrated ambient conditions, with the only difference being the amount of layers due to increases in growth rate, it can be assumed that if recrystallization occurs it is a result of increased mineral layering. Calcite 120 and calcite 60 were chosen for resuspension experiments because they exhibited the least amount of layering, the subtle changes in roughness and growth rate were then tested against recrystallization as described in the next section.

Resuspension Experiments

Table.5 demonstrates the conversion of raw radioactive data into the more commonly expressed terminology, becquerels (Bq). Since the radioactivity detector reports the quantity of disintegrations in the form of count rate, it is necessary to determine the detector efficiency to see how many disintegrations the instrument is capable of detecting. The counts per minute must be converted into becquerels, as that is the measure of disintegrations per second that is simply dependent on the quantity of isotope. The following calculation was followed to obtain efficiency (https://www.perkinelmer.com/lab-products-and-services/application-support-knowledgebase/radiometric/radiochemical-calculations.html):

Efficiency = Net CPM of standard / Known DPM of standard. (Eq. x)

Known disintegrations per minute, DPM, is determined by multiplying the known activity of the standard solution by 60 (400Bq * 60 = 23976 dpm). The net counts per minute, CPM, of the standard blank solution obtained from the detector is 14652. The efficiency of the detector is 61% (14652 cpm / 23976 dpm = 0.611). All CPM values from the detector were converted to DPM by dividing by the efficiency as well as dividing by 60 to get the unit becquerels.

Results of the four ^{45}Ca radiotracer experiments are summarized in Figures 9 & 10. The initial ^{45}Ca activity in all batches, with and without calcite, is 400 $BqmL^{-1}$. Over 106 days, all four experiments demonstrate a steady decline of $^{45}Ca_{(aq)}$, that is attributed to the natural decay of the isotope and not to the uptake of ^{45}Ca into the solid (Fig. 9a). The total $^{45}Ca_{(aq)}$ drops by approximately half over the course of the reaction, these

results correlate well with the half-life of the radioisotope. The average $^{45}Ca_{(aq)}$ activity from each batch experiment (Fig. 9b) was plotted versus time, expressed as fractions of total added ^{45}Ca (400 $BqmL^{-1}$) (Fig. 9c). The data for total ^{45}Ca are taken from the series of control samples that were prepared without solid, this was used to correct for decay. All four experiments show no evidence of ^{45}Ca incorporation over the experimental time period, with total calcium remaining constant. Figure 10 is the same data as presented in Figure 9c, except separated by the extrinsic variable pH. The data points that are along the red dashed line, 1.0±0.2, in Fig. 10a indicate the ^{45}Ca concentration is at equilibrium for both samples of calcite 120 (faster growth rate) at pH 8.3. Similar results for calcite 60 (slower growth rate), resuspended under identical conditions, can be seen in Fig. 10b. Thus, the intrinsic variable, growth rate differences, are not correlated with ^{45}Ca uptake in the experiments. The data for samples of calcite 120 at pH 7.5 (Fig. 10c), are also scattered along the fraction of 1.0 (red dashed line), meaning that the 1:1 ratio between concentration of aqueous calcium and solid calcium are maintained as both parts undergo same rate of change. Regardless of the extrinsic variable, pH, calcite 120 and calcite 60 at pH 8.3 (Fig.10a & b) compared to calcite 120 and calcite 60 at pH 7.5 (Fig.10c & d), both are at dynamic equilibrium with no discernible change in calcium concentration. Each batch of experiments undergoes dissolution and precipitation at the same rate, resulting in a dynamic exchange.

Parallel stable isotope reactors used to detect changes in aqueous concentrations were evaluated at the same time points as the radioactive isotope reactors. Results of the four stable isotope experiments can be seen in Figures 11 & 12. Synonymous to data from the radioactive experiments (Fig. 10c), over 106 the aqueous Ca^{2+} concentration

remains at the fraction 1.0 (Fig.11c), indicating the aqueous solid 1:1 ratio remains constant. Similarly, growth rate differences do not affect rate of calcium exchange or extent of exchange as is evidenced by Fig. 12a & 12b, and Fig.12c & 12d. The stable isotope reactors also do not show differences in affects due to pH. Both calcite 120 and calcite 60 are in dynamic equilibrium regardless of growth rate differences or pH. However, when looking at total calcium from batch experiments including the blanks (without solid), there is an increase during the initial 18 days, which then levels off (Fig. 11a & 11b).

Discussion

The abundance and solubility of calcite means that the system exerts a very strong control on the surrounding aqueous chemistry. The mineral stability has been the focus of many experimental studies, as this process has important implications for the mineral lattice being open to exchange. The exchange of calcite with other atoms from its surroundings can be near the surface layers or into the bulk mineral lattice, the driving force of calcite exchange under equilibrium conditions and low temperature settings remains a debate. Because calcite serves as a means of immobilizing pollutants, it is important to study it's static/non-static nature. Previous physiochemical parameters do not take into account the recrystallization of calcite with respect to pH and initial growth rate, as will be done in this discussion. Conclusions based on batch recrystallization experiments are variable because of 1) the difficulty in quantifying recrystallization 2) the many different approaches to testing recrystallization. The current experiments offer information to add to the interpretation of the kinetics behind the stability of calcite.

The Role of Growth Rate on Calcite Recrystallization

Interpretation of the results is based on the data of precipitation rate combined with measurements of radiotracer calcium during the resuspension portion of the experiments. Under the conditions tested, there is no evidence of equilibrium isotopic change, therefore during resuspension, all systems undergo precipitation and dissolution at the same rate (Fig.13). Calcite 120, 60, and 30 show the formation of chemically

homogeneous precipitation overgrowths (Fig.8), with increasing overgrowths as a result of decreasing precipitation rate (Fig.14).

The relationship between overgrowths and surface crystallinity depends on surface defects such as porosity, hillocks and steps. The less defects there are, the more crystalline a surface is, the less surface energy it has. Although this study does not focus on individual surface defects, it does rely on the amount of crystallinity of each calcite to give us an overall sense of surface smoothness. Given that calcite crystal grows with each individual layer accumulating on top of each other in progression, the surface of each layer eventually becomes the bulk of the crystal as it grows. This in turn means that if there were defects in the surface, there are defects in the bulk of the calcite crystal.

Results from previous authors have suggested that crystal defects are the driving force of mineral recrystallization under conditions that satisfy calcite equilibrium. In the present experiments, the variable of growing calcite at different rates was demonstrated to overcome the limitation of surface defects. With a decrease in growth rate and increase in overgrowths, surface defects according to the full width half maximum (fwhm) do not increase (Table 6.). There is evidence of a wider value of fwhm that belongs to a duplicate sample of Calcite 60, this could have been due to a packing error that caused an artefact in the XRD data. All other values fall within a small range of 0.13-0.17, indicating surface smoothness is not affected by increase in precipitation rate. There are no major surface defects in the calcite crystals and none notable enough to produce a driving force for recrystallization as demonstrated by the resuspension experiments. Surface reactivity influenced by properties of porosity, surface defects and size distribution may have been minimized during the growth process by a factor of a good

calcium to carbonate ratio, having no inhibitors of growth and maintaining adequate pH for proper stabilization of aqueous equilibrium during the growth process. The results demonstrate that small defects, if present, are not significant enough to produce a driving force for recrystallization. Diminishing crystal defects during precipitation lessens the energy of the bulk mineral needed for recrystallization.

Variables Controlling Calcite Stability

In terms of kinetics, all calcite systems are close enough to equilibrium to maintain mineral stability for the time period examined. Although dynamic equilibrium is maintained, it could take longer time scales to detect if there is a change in the rates of equilibrium. While recrystallization derived from geogenic timescales has not yet been studied for calcite, according to a study done with barite, complete bulk barite equilibration can take up to 1400 – 16,900 years (Heberling at al., 2018). Evaluation of calcite recrystallization kinetics also depends solid/liquid ratios. Curti et al. (2005) demonstrated that for calcite, it is not possible to determine recrystallization rate at 0.5 g L^{-1} because of the very weak uptake of ^{45}Ca. During the first portion of our experiments greater amounts of calcite than the 20 mg L^{-1} for calcite at pH 8.3 and 728 mg L^{-1} for pH 7.5 used, is required for a stronger signal of uptake. Thus, the processes of recrystallization could not be fully discerned because higher solid liquid ratios (S/ L) are needed for higher exchange site availability.

The Role of pH on Calcite Recrystallization

Findings based on pH during the resuspension portion of the experiments reflect changes in mineral chemistry, however subtle they may be, to indicate if there is recrystallization occurring. Such changes differ from those described in the section above because differences in pH would be due to mineral and aqueous chemistry as opposed to mineral morphology. Evidence of chemical changes include changes in pH and differences in radioisotope vs. stable isotope uptake. For evidence of isotope exchange due to pH, we note ^{45}Ca radioisotope exchange values are the same for each pH and the same statement can be said for the stable ^{40}Ca exchange values. Table 7. demonstrates the variation in solution pH during stable ^{40}Ca exchange, for experiments of pH=7.5 there is a decrease in pH of about 0.2, whereas for experiments that began at pH=8.3, there is a decrease of 0.4-0.7. Although stable isotope exchange experiments under pH=7.5 have a more stable solution pH throughout the course of the experiment than the experiments under pH=8.3, a change in pH is not uncommon and is still insufficient to produce dissolution. It can also be seen that at Day 78 there is a noticeable lower pH in all pH=8.3 and pH=7.5 samples than in any other day. The variability in this pH data is, likely, a random measurement error rather than an indication of recrystallization. This means that, even with variations in pH, the experimental systems still reflect dynamic equilibrium.

Radioisotope vs. Stable Isotope Uptake

Results of ^{45}Ca radioisotope exchange demonstrate that equilibrium is maintained throughout the duration of the experiment for both experiments under pH= 8.3 and

pH=7.5 indicating the stability of calcite is positively correlated with dynamic equilibrium. With respect to our data, results suggest the possibility that stable isotope exchange could outcompete radioisotope exchange due to slight differences in fractionation demonstrated by the scattering of the radioisotope concentrations data over time. As previously mentioned, stable ^{40}Ca exchange demonstrates dynamic equilibrium being reached, but with an overall closer approximation for both pH= 8.3 and pH=7.5 when compared to ^{45}Ca radioisotope exchange. Less scatter is observed for the ^{40}Ca isotope, with a closer approximation to 1, suggesting that the stable isotope experiments with the lighter isotope reacts more readily than the radioisotope experiment with the heavier isotope. This is likely due to mass dependent isotope fractionation, which are the subtle variations in behavior caused by the differences in mass between isotopes of the same element (Ryan., 2014). Molecules with lighter isotopes are broken easily because the bond is less stable and requires less energy to break, therefore a lighter isotope will react more rapidly than a molecule with a heavier isotope (Ryan et al., 2014., USGS website). In the case of the ^{45}Ca radioisotope exchange, sample plots were a bit further from 1 than indicating the heavier isotope could preferentially partition to calcite relative to the aqueous solution and is a bit further from equilibrium compared to stable ^{40}Ca exchange.

A previous experimental investigation done by Oelkers et al (2019) supports the idea of isotope fractionation occurring in calcite systems that are not fully in bulk chemical equilibrium. The study done by Oelkers et al (2019), in which stable Ca isotopes were used for calcite at ambient temperature during its dissolution, precipitation, and at equilibrium in week long closed system experiments, resulted in close to complete

isotopic equilibrium only after the system attained full dynamic equilibrium. This former study implies that for isotopic signatures to be preserved in calcite, the system must be closed, and dynamic equilibrium must be reached. This conclusion implies that the calcite in the present study may be in full bulk chemical equilibrium since we note isotope fractionation, although detectable, is not significant enough to be considered fractionated.

The variability in ^{45}Ca vs. ^{40}Ca measurements is most probably, due to analytical error, as it cannot entirely be attributed to mass fractionation. Analytical error is when measurements deviate slightly low or slightly high from the average value, which is what it seen in the ^{45}Ca measurements. The analytical error in the resuspension experiments is due to the sensitivity of the instruments used for each experiment. The ^{40}Ca measurements taken with the spectroscopic method of ICP-OES involves the atomization of the sample after aspirating it into an argon plasma torch at 6000 – 8000 K. This procedure produces an intense emission that is clean and free of most interferences, resulting in high efficiency and sensitivity (Kebbekus B.B, Mitra S., 1998). Such high sensitivity results in the higher analytical precision evidenced in the ^{40}Ca measurements. The ^{45}Ca measurements were taken with a different instrument that involves liquid scintillation counting. The liquid scintillation counting method requires the radioactive molecule + solvent molecule + scintillators to produce energy in the form of light, which is then detected by the photomultiplier tube of the liquid scintillation counter (Perkin Elmer). Although this method is also sensitive, quenching could occur, a process in which the energy emitted by a radioisotope is not transferred completely into light and therefore is not detected by the counting instrument. This results in a decrease in the final

signal, additionally when compared to the ICP-OES, the liquid scintillation counting instrument is more rugged in terms of the ease with which good results are produced.

On the contrary to Oelkers et al (2019), a recent study, done by Heberling et al (2018), implies that using different isotopes does not affect recrystallization. The study argues that what truly moves recrystallization to a slower rate is the increase in pre-equilibration times in laboratory experiments, although still considered fast when compared to geological times. In their experiments, other variables like pH, S/L ratio, and ion ratios are only minor when related to recrystallization rates. For the present study S/L ratios do play a significant role in terms of detecting concentration ratios related to equilibration. The Heberling et al (2018) experiment consisted of long-term batch type experiments with barite and although they used a more reactive mineral, their experimental set up and long-term usage of isotopes is very similar to the current study presented, implying that longer pre-equilibration times could further maintain equilibrium. Similarly, for the current experiments, by adequately growing calcite the system could further maintain equilibrium. Further experimentation with higher S/L ratios is necessary in order to decide whether using different isotopes are indeed not related to recrystallization. The experiments conducted in this study first aim to grow calcite through precipitation to examine if different growth rates change the minerals morphology, thus affecting crystal surfaces and in turn causing it to be a possible driving force for recrystallization. Experimental results show that there was no change in morphology or crystallinity due to differences in growth rate, although there was an observed increase of overgrowths. The data shows no evidence that increase in overgrowths affect the mineral's crystallinity or stability once it is resuspended in its

ideal solution. It is possible that selecting samples with greater differences in overgrowths, such as calcite 120 vs calcite 30, instead of the studied calcite 120 vs calcite 60, could reflect results with stronger correlation between growth rate and calcite stability. The second aim of this study was to assess the role different pH's have on calcite stability during resuspension. According to the results, even with minor drifts of pH in each experiment, dynamic equilibrium is maintained for both pH 8.3 and pH 7.5, implying that small changes in pH within the studied range is not a strong variable in determining calcite stability.

Results from the experiments do not explain the hypothesized calcite recrystallization, rather they demonstrate trends related to dynamic equilibrium. The findings in this study, while preliminary, provide an opportunity to advance the understanding of calcite stability by suggesting that the systems a) rates of formation are affected by rate of delivery of constituent ions (syringe pump rate), b) overgrowths increase with decreasing growth rates and c) more overgrowths is not indicative of lower crystallinity d) high S/L ratios are needed for strong signal uptake. The question remains, can a non-reactive mineral such as calcite show evidence of recrystallization under apparent equilibrium conditions? In order to come to a conclusion to this question, further investigation is necessary.

Conclusion

The reported results of the current experiments demonstrate that, once calcite is re-suspended in solution, dynamic equilibrium is maintained, in which the solid and the solution remain stable under constant dissolution and precipitation. Crystal growth could play a role in maintaining equilibrium. Crystallinity remained in its existing condition during the growth process even with an observed increase in overgrowths. The occurrence of calcite overgrowths increases at lower calcite growth rates, such correlation can be used to estimate mineral growth rates. This growth mechanism has the possibility of decreasing surface defects, thus diminishing surface reactivity as a driving force for recrystallization. The main supporting evidence that the crystals in the current experiment are resistant to recrystallization is found in the constant concentration of radio isotope and stable isotope over time, thus having constant rate over time. A closer estimation of calcium concentration was detected in stable isotope experiments; however, these results are attributed to using a more precise analytical instrument than in the radio isotope experiments. In the case of pH, there is no discernible correlation between the system pH and recrystallization, this is a minor variable. A variable concerning the detectability of recrystallization is that of the S/L ratio, as a higher S/L ratio is necessary for positive results. The conclusions presented have implications for using calcite as an effective mineral for contaminant retention. Whether calcite has atoms deep within the mineral lattice that can readily exchange with surroundings cannot be concluded in the present study and has to be analyzed in future work in which calcite grown with alternating layers of radio isotope and stable isotope is subjected to resuspension.

Future Work

The results of the current study do not support our hypothesis on the selected two variables, pH and initial calcite growth rate, effecting calcite stability. Answering the question on whether calcite recrystallization occurs at near bulk chemical equilibrium conditions and what is the driving force that allows such a mechanism to occur requires further assessment. To begin with, refining the current experimental methods by increasing S/L ratios to assess higher calcite loadings. Higher loadings allow stronger radio isotope and stable isotope signals that can detect the extent of isotope fractionation. Additionally, providing scanning electron microscopy (SEM) images of the calcite crystals will help reveal the particle morphology by the end of the resuspension experiment. Complete microscopic imaging information gives implications on the connection between crystal surface morphology and recrystallization. Calcite at close to bulk equilibrium conditions may be resistant to recrystallization even with subtle changes in growth rates. Further experiments in which initial growth rates vary greatly could provide results more in line with previous studies that imply surface morphology impacts recrystallization. Finally, in order to quantify the extent of recrystallization from within the calcite mineral, future work requires a more advanced isotopic analysis. By growing calcite with alternating layers of radio isotope and stable isotope (Fig.15), isotopes from within the bulk layers of the mineral can be monitored to exchange with the aqueous solution.

References

Ahmed I.A.M, Crout N. M.J and Young, S.D. (2009) Kinetics of Cd sorption, desorption and fixation by calcite: A long-term radiotracer study. *Geochim. Cosmochim. Acta* **72,** 1498– 1512

Alkattan M., Oelkers E.H., Dandurand J., Schott J. (2002) An experimental study of calcite dissolution rates at acidic conditions and 25C in presence of $NaPO_3$ and $MgCl_2$. *Chem Geol* **190,** 291-302

Aquilano D., Calleri M., Matoli E., Rubbo M., Sgualdino G. (2000) The {104} cleavage rhombohedron of calcite: theoretical equilibrium properties. *MatChemPhys* **66** 59-163

Avrahamov N., Sivan O., Yechieli Y., Lazar B. (2013) Carbon isotope exchange during calcite interaction with brine: Implications for 14C dating of hypersaline groundwater. *Radiocarbon* **55** 81-101

Aziz H.A., Adlan M.N., Ariffin K.S. (2007) Havy Metals (Cd, Pb, Zn, Ni, Cu and Cr (III)) removal from water in Malaysia: Post treatment by high quality limestone. *Bioresea.Tech.* **99,** 1578-1583

Berner R.A (1975) The role of magnesium in the crystal growth of calcite and aragonite from sea water. *Geochim. Cosmochim. Acta* **39,** 489-494

Bozlee B.J. and Janebo M. (2008) A simplified model to predict the effect of increasing atmospheric CO_2 on carbonate chemistry in the ocean. *J.Chem Edu* **85** 213-217

Brantley S.L., Kubicki J.D., White A.F. (2008) Kinetics of water-rock interaction. New York, NY: Springer

Cubillas P. and Anderson M.W. (2010) Zeolites and Catalysis, Synthesis, Reactions and Applications. *Wiley* **1**

Curti E., Kulik D.A., Tits J. (2005) Solid solutions of trace Eu(III) in calcite: Thermodynamic evaluation of experimental data over a wide range of pH and pCO_2. *Geochim. Cosmochim. Acta* **69,** 1721-1737

Cravotta III C.A and Trahan M.K (1999) Limestone drains to increase pH and remove dissolved metals from acidic mine drainage. *Appl Geochem* **14,** 581-606

Davis J.A., Fuller C.C, Cook A.D. (1987) A model for trace metal sorption processes at the calcite surface: Adsorption of Cd^{2+} and subsequent solid solution formation. *Geochim. Cosmochim. Acta* **51,** 1477-1490

Davis K.J., Dove P.M., Wasylenki L.E., De Yoreo J.J. (2004) Morphological consequences of differential Mg^{2+} incorporation at structurally distinct steps on calcite. *Amer Miner*. **89,** 714-720

Eby N.G. (2004) *Principles of environmental geochemistry*. Pacific Grove, CA: Brooks/Cole-Thomas Learning.

Elzinga E.J., Rouff A.A., Reeder R.J. (2006) The long- term fate of Cu^{2+}, Zn^{2+}, and Pb^{2+} adsorption complexes at the calcite surface: An X-ray absorption spectroscopy study. *Geochim. Cosmochim. Acta* **70,** 2715-2725

Feely R.A., Sabine C.L., Lee K., Berelson W., Kleypass J., FabryV.J., Millero G.J. (2004, July) Impact of anthropogenic CO_2 on the $CaCO_3$ system in the oceans. *Science.Mag.* **305,** 362-366

Gao Z., Li C., Sun W., Hu Y. (2017) Anisotropic surface properties of calcite: A consideration of surface broken bonds. *J.ColSurfa* **520** 53-61

Gorski C.A, Fantle M.S (2017) Stable mineral recrystallization in low temperature aqueous systems: A critical review. *Geochim. Cosmochim. Acta* **198,** 439-465

Heberling F., Denecke M.A., Bosbach D. (2008) Neptunium(V) coprecipitation with calcite. *Environ. Sci. Technol* **42** 471-476

Heberling F., Bosbach D., Eckhardt J-D., Fischer U., Glowacky J., Haist M., Kramar U., Loos S., Müller H.S., Neumann T., Pust C., Schäfer T., Stelling J., Ukrainczyk M., Vinograd V., Vučak M., Winkler B. (2014) Reactivity of the calcite–water-interface, from molecular scale processes to geochemical engineering. *J.ApGeoChem* **45** 158-190

Heberling F., Pauling L., Nie Z., Schild D., Fink N. (2016) Morphology controls on calcite recrystallization. *Environ. Sci. Technol* **50** 11735-11741

Inks C.G and Hahn R.B. (1967) Determination of surface area of calcium carbonate by isotopic exchange. *Analyt. Chem* **39,** 625-628

Heberling F., Metz V., Böttle M., Curti E., Geckels H. (2018) Barite recrystallization in the presence of ^{226}Ra and ^{133}Ba. *Geochim. Cosmochim. Acta* **232,** 124-139

Ibrahim A-R., Vuningoma J.B., Hu X., Gong Y., Hua D., Hong Y., Wong H., Li J. (2012) High-pressure gas-solid carbonation route coupled with a solid ionic liquid for rapid synthesis of rhombohedral calcite. *J.SupFlu* **72** 78-83

Inks C.G and Hahn R.B. (1967) Determination of surface area of calcium carbonate by isotopic exchange. *Analyt. Chem* **39,** 625-628

Jacob J.J., Valarkshmi R., Jayasri M.A., Suthindhiran K. (2018) Removal of Cr(III) and Ni (II) from tannery effluent using calcium carbonate coated bacterial magnetosomes, *Nature Partn Journ* 1:1

Kebbekus B.B, Mitra S. (1998) *Environmental chemical analysis*. Boca Raton, Florida: Chapman & Hall/ CRC

Land P.E., Shutler J.D., Findlay H.S., Girard-Ardhuin F., Sabia R., Reul N., Piolle J., Chapron B., Quilfen Y., Salisbury j., Vandemark D., Bellerby R., Bhadury P. (2015) Salinity from space unlocks satellite-based assessment of ocean acidification. *Environ. Sci. Technol* **49** 1987-1994

Langmuir D. (1997) *Aqueous Environmental Geochemistry*. Upper Saddle River, NJ: Prentice-Hall; Inc.

Lakshtanov L.Z., Belova D.A., Okhrimenko D.V., Stipp S.L.S. (2015) Role of alginate in calcite recrystallization. *J. Cryst. Growth* **15,** 419-427

Larsen K., Bechgaard K., Stipp S.L.S. (2010) The effect of the Ca^{2+} to CO_3^{2-} activity ratio on spiral growth at the calcite {1014} surface. *Geochim. Cosmochim. Acta* **74,** 2099-2109

Lasaga A.C. and Blum A.E. (1986) Surface chemistry, etch pits and mineral-water reactions. *Geochim. Cosmochim. Acta* **50,** 2363-2379

Liang L., Heveran C., Liu R., Gill R.T., Nagarajan A., Cameron J., Hubler M., Srubar III W.V., Cook S. (2018) Rational control of calcium carbonate precipitation by engineered *Escherichia Coli. ACS Synth* Biol **7,** 2497-2506

Massaro F.R., Pastero L., Rubbo M., Aquilano D. (2008) Theoretical surface morphology of {011¯2} acute rhombohedron of calcite: A comparison with experiments and {101¯4} cleavage rhombohedron. *J. Cryst. Growth* **310** 706-715

Mavromatis V., Immenhauser A., Buhl D., Purgstaller B., Baldermann A., Dietzel M. (2017) Effect of organic ligands on Mg partitioning and Mg isotope fractionation during low-temperature precipitation of calcite in the absence of growth rate effects. *Geochim. Cosmochim. Acta* **207** 139-153

Moller P., and Sastri C.S. (1973) Exchange studies on single crystals of calcite using ^{45}Ca as the tracer. *Inorg. Nucl. Chem. Letters* **9,** 759-763

Moreno A., Ruiz-Arellano R.R. (2014) Obtainment of spherical-shaped calcite crystals induced by intramineral proteins isolated from eggshells of ostrich and emu. *Cryst Growth Des* **14** 5137-5143

Morse J.W., Arvidson R.S., Luttge A. (2007) Calcium carbonate formation and dissolution. *Chem. Rev* **107,** 342-381

Mozeto A.A., Fritz P, Reardon E.J. (1984) Experimental observations on carbon isotope exchange in carbon-water systems. *Geochim. Cosmochim. Acta* **48,** 495-504

Mucci A. and Morse J.W. (1983) The incorporation of Mg^{2+} and Sr^{2+} into calcite overgrowths: influences of growth rate and solution composition. *Geochim. Cosmochim. Acta* **47,** 217- 233

Oelkers E.H., Pogge von Strandmann P.A.E., Mavromatis V. (2019) The rapid resetting of the Ca isotope signatures of calcite at ambient temperature during its congruent dissolution, precipitation, and at equilibrium. *Chem Geol* **512,** 1-10

Perkin Elmer. Radiochemical calculation Retrieved from https://www.perkinelmer.com/lab-products-and-services/application-support-knowledgebase/radiometric/radiochemical-calculations.html

Perkin Elmer. Liquid Scintillation Counting Method Retrieved from https://www.perkinelmer.com/lab-products-and-services/application-support-knowledgebase/radiometric/liquid-scintillation-counting.html

Phreeqc 3.1.7. Retrieved from https://www.usgs.gov/software/phreeqc-version-3.

Plummer L.N., Wigley T.M.L., Parkhurst D.L. (1978) Kinetics of calcite dissolution in CO_2 – water systems at 5 degree to 60 degree C and 0.0 to 1.0 atm CO_2. *Am.J.Sci* **278** 179-216

Plummer L.N. and Busenberg E. (1982) The solubilities of calcite, aragonite and vaterite in CO_2-H_2O solutions between 0 and 90°C, and an evaluation of the aqueous model for the system $CaCO_3$-CO_2-H_2O. *Geochim. Cosmochim. Acta* **46** 1011-1040

Reeder R.J. (1983) *Carbonates: mineralogy and chemistry*. Washington, D.C: Mineralogical Society of America.

Reddy M.M.and Gillard W.D. (1981) Kinetics of calcium carbonate (calcite)-seeded crystallization: influence of solid/solution ratio on the reaction rate constant. *J. Colloid Interface Sci.* **80,** 171-178

Reddy M.M.and Nancollas G.H. (1971) The crystallization of calcium carbonate I. Isotopic exchange and kinetics. *J. Colloid Interface Sci.***36,** 166-172

Reeder R.J. (1983) The kinetics of calcium carbonate dissolution and precipitation. In Morse J.W, *Carbonates: Mineralogy and chemistry* (pp.227-264). Mineralogical Society of America.

Reeder R.J., Elzinga E.J., Tait C.D., Rector K.D., Donohoe R.J., Morris D.E. (2004) Site-specific incorporation of uranyl carbonate species at the calcite surface. *Geochim. Cosmochim. Acta* **68,** 4799-4808

Rouff A.A., Elzinga E.J., Reeder R.J., Fisher N.S. (2005) The influence of pH on the kinetics, reversibility and mechanisms of Pb(II) sorption at the calcite-water interface. *Geochim. Cosmochim. Acta* **69,** 5173– 5186.

Ryan P.C. (2014) *Environmental and low temperature geochemistry.* West Sussex, UK: John Wiley & Sons

Sand K.K., Tobler D.J., Dobberschutz S., Larsen K.K., Makovicky E., Andersson M.P., Wolthers M., Stipp S.L.S. (2016) Calcite growth kinetics: Dependence on saturation index, Ca^{2+}:CO_3^{2-} activity ratio, and surface atomic structure. *J. Cryst. Growth* **16,** 3602-3612

Stipp S.L.S., Konnerup-Madsen J., Franzreb K., Kulik A., Mathieu H.J., (1998) Spontaneous movement of ions through calcite at standard temperature and pressure. *Nature* **396,** 356-359

Tang H., Xian H., He H., Wei J., Liu H., Zhu J., Zhu R. (2019) Kinetics and Mechanisms of the interaction between the calcite (10.4) surface and Cu^{2+} -bearing solutions. *Sci.ofTot.Envi.* **668,** 602-616

Teng H.H., Dove P.M., Yoreo J.J. (2000) Kinetics of calcite growth: Surface processes and relationships to macroscopic rate laws. *Geochim. Cosmochim. Acta* **64** 2255-2266

Tertre E., Page J., Beaucaire C. (2012) Ion exchange model for reversible sorption of divalent metals on calcite: Implications for natural environments. *Environ. Sci. Technol* **46,** 10055-10062

Tertre E., Beaucaire C., Juery A., Ly J. (2010) Methodology to obtain exchange properties of the calcite surface—Application to major and trace elements: Ca(II), HCO_3, and Zn(II). *J. Colloid Interface Sci* **347,** 120-126

Tesoriero A.J. and Pankow J.F. (1996) Solid solution partitioning of Sr^{2+}, Ba^{2+}, and Cd^{2+} to calcite. *Geochim. Cosmochim. Acta* **60,** 1053-1063

United States Geological Survey USGS. Retrieved from https://wwwrcamnl.wr.usgs.gov/isoig/isopubs/itchch2.html

Visual MINTEQ 3.1. Retrieved from https://www.kth.se/

Zachara J.M., Cowan C.E., Resch C.T. (1991) Sorption of divalent metals on calcite. *Geochim.Cosmochim. Acta* **55,** 1549-1562

Zhong S. and Mucci A. (1993) Calcite precipitation in seawater using a constant addition technique: A new overall reaction kinetic expression. *Geochim. Cosmochim. Acta* **57,** 1409-1417

Appendix A: Tables

Table.1 Calcite saturation index above zero for supersaturation and growth. Calculation run in Visual MINTEQ 3.1.

Mineral	log IAP	Sat. index
Aragonite	-8.292	0.044
CaCO3xH2O(s)	-8.293	-1.149
Calcite	-8.292	0.188
Lime	13.277	-19.422
Natron	-7.042	-5.731
Portlandite	13.276	-9.428
Thermonatrite	-7.029	-7.666
Vaterite	-8.292	-0.378

Table.2 PHREEQC output. Calculations for the amount of calcium needed for calcite growth experiment.

a) PHREEQC calcium calculations for pH 8.3

```
-------------------------------Phase assemblage-------------------------------

                                        Moles in assemblage
Phase               SI log IAP  log KT      Initial       Final       Delta

Calcite            0.00   -8.48   -8.48    1.000e+01   9.999e+00  -8.212e-04
CO2(g)            -3.40   -4.87   -1.47    1.000e+01   9.999e+00  -7.794e-04

-----------------------------Solution composition-----------------------------

            Elements          Molality       Moles

            C                1.601e-03   1.601e-03
            Ca               8.212e-04   8.212e-04
            N                1.000e-01   1.000e-01
            Na               1.000e-01   1.000e-01

----------------------------Description of solution----------------------------

                                pH  =   8.285      Charge balance
                                pe  =  11.340      Adjusted to redox equilibrium
      Specific Conductance (uS/cm, 25 oC) = 10443
                        Density (g/cm3)  =   0.99801 (Millero)
                     Activity of water  =   0.997
                      Ionic strength  =   1.024e-01
                    Mass of water (kg)  =   1.000e+00
               Total alkalinity (eq/kg)  =   1.642e-03
                   Total CO2 (mol/kg)  =   1.601e-03
                  Temperature (deg C)  =  25.000
                Electrical balance (eq)  =  -1.486e-08
 Percent error, 100*(Cat-|An|)/(Cat+|An|)  =  -0.00
                          Iterations  =  33
                            Total H  = 1.110124e+02
                            Total O  = 5.581024e+01
```

Table.2

b) PHREECQ calcium calculations for pH 7.5

```
-----------------------------Phase assemblage-----------------------------

                                                    Moles in assemblage
Phase               SI log IAP  log KT      Initial       Final       Delta

Calcite           0.00   -8.48   -8.48    1.000e+01   9.963e+00  -3.702e-02
CO2(g)           -3.40   -4.87   -1.47    1.000e+01   1.004e+01   3.670e-02
fix_H+           -7.50   -7.50    0.00
          HNO3              is reactant      1.000e+01   9.926e+00  -7.373e-02

----------------------------Solution composition----------------------------

          Elements          Molality       Moles

          C                3.220e-04   3.222e-04
          Ca               3.700e-02   3.702e-02
          N                1.736e-01   1.737e-01
          Na               9.993e-02   1.000e-01

---------------------------Description of solution---------------------------

                                pH  =   7.500      Charge balance
                                pe  =  12.267      Adjusted to redox equilibrium
      Specific Conductance (uS/cm, 25 oC) = 16804
                        Density (g/cm3)  =   0.99884 (Millero)
                     Activity of water  =   0.995
                       Ionic strength  =   2.108e-01
                    Mass of water (kg)  =   1.001e+00
                Total alkalinity (eq/kg)  =   3.163e-04
                    Total CO2 (mol/kg)  =   3.220e-04
                   Temperature (deg C)  =  25.000
                 Electrical balance (eq)  =  -1.484e-08
 Percent error, 100*(Cat-|An|)/(Cat+|An|)  =  -0.00
                           Iterations  =  25
                             Total H  = 1.110862e+02
                             Total O  = 5.606507e+01
```

Table.3 Calcite average growth properties: pH over time and Rates calculated based on change in calcium concentration over time.

	Calcite 120 uL/min				Calcite 60 uL/min				Calcite 30 uL/min			
Time	**Sample**	**pH**	**avg [Ca]ppm**	**Growth Rate (mol/s)**	**Sample**	**pH**	**avg [Ca]ppm**	**Growth Rate (mol/s)**	**Sample**	**pH**	**avg [Ca]ppm**	**Growth Rate (mol/s)**
0	0	8.18	4.595	-5.67	0	8.25	4.54	-5.97	0	8.12	4.675	-6.27
2	1	8.675	5.78	-9.53	1	8.625	5.425	-9.83	1	8.405	4.9	-10.13
4	2	8.53	6.5	-9.83	2	8.535	5.715	-10.13	2	8.36	5.11	-10.43
8	3	8.405	6.435	-10.13	3	8.46	6.47	-10.43	3	8.32	5.14	-10.73
17	4	8.6	8.315	-10.46	4	8.345	7.035	-10.76	4	8.41	4.32	-11.06
24					5	8.52	7.935	-10.91	5	8.5	4.825	-11.21
33					6	8.365	7.25	-11.06	6	8.415	4.915	-11.35
49									7	8.38	5.47	-11.52
65									8	8.445	6.04	-11.64

Table.4 Calcium concentrations for calcite grown at syringe pump rate of 120 µL/min, 60 µL/min and 30 µL/min. Compositions for each calcite and their duplicate are shown.

Time (h)	Sample #	Calcite 120 Ca (ppm)	Calcite 120-1 Ca (ppm)	Calcite 60 Ca (ppm)	Calcite 60-1 Ca (ppm)	Calcite 30 Ca (ppm)	Calcite 30-1 Ca(ppm)
0	Sample-0	4.52	4.67	4.52	4.56	4.88	4.47
2	Sample-1	5.68	5.88	5.28	5.57	5.25	4.55
4	Sample-2	6.55	6.45	5.5	5.93	5.45	4.77
8	Sample-3	6.65	6.22	6.5	6.44	4.92	5.36
17	Sample-4	7.56	9.07	7.12	6.95	3.11	5.53
24	Sample-5			8.17	7.7	3.78	5.87
33	Sample-6			7.59	6.91	3.82	6.01
49	Sample-7					4.5	6.44
65	Sample-8					4.98	7.1

Table.5 Calculations of radio isotope concentration units in Counts Per Minute converted to Becquerels

a) Calcite 120 & 60 resuspended in a pH 8.3 equilibrated solution, calculations of CPM to Bq

	Calcite 120 Control			Calcite 120 Sample 1			Calcite 120 Sample 2			Calcite 60 Control			Calcite 60 Sample 1			Calcite 60 Sample 2		
Time (days)	cpm	dpm	Bq	cpm	dpm	Bq	cpm	dpm	Bq	cpm	dpm	Bq	cpm	dpm	Bq	cpm	dpm	Bq
0	14652.00	23980.36	399.67	12185.40	19943.37	332.39	12355.40	20221.60	337.03	13709.40	22437.64	373.96	13096.80	21435.02	357.25	10369.80	16971.85	282.86
1	13212.40	21624.22	360.40	13659.80	22356.46	372.61	13458.20	22026.51	367.11	14364.20	23509.33	391.82	13462.20	22033.06	367.22	13253.00	21690.67	361.51
2	12765.60	20892.96	348.22	13236.40	21663.50	361.06	12784.60	20924.06	348.73	11767.60	19259.57	320.99	13949.00	22829.79	380.50	12135.60	19861.87	331.03
3	14068.80	23025.86	383.76	14854.40	24311.62	405.19	14553.60	23819.31	396.99	14542.00	23800.33	396.67	13523.20	22132.90	368.88	12517.80	20487.40	341.46
4	14266.80	23349.92	389.17	14806.40	24233.06	403.88	14485.40	23707.69	395.13	14140.60	23143.37	385.72	14297.20	23399.67	389.99	12873.00	21068.74	351.15
6	13565.20	22201.64	370.03	14429.60	23616.37	393.61	14206.00	23250.41	387.51	13777.20	22548.61	375.81	12451.60	20379.05	339.65	14421.40	23602.95	393.38
10	12911.20	21131.26	352.19	13332.80	21821.28	363.69	12137.80	19865.47	331.09	13479.80	22061.87	367.70	13353.40	21854.99	364.25	13306.80	21778.72	362.98
15	12848.60	21028.81	350.48	13908.80	22763.99	379.40	13675.40	22382.00	373.03	12888.60	21094.27	351.57	12549.60	20539.44	342.32	12510.60	20475.61	341.26
22	11517.20	18849.75	314.16	13211.40	21622.59	360.38	11638.40	19048.12	317.47	12549.00	20538.46	342.31	12438.60	20357.77	339.30	11689.80	19132.24	318.87
29	9023.20	14767.92	246.13	9399.20	15383.31	256.39	10982.00	17973.81	299.56	11487.40	18800.98	313.35	11867.20	19422.59	323.71	11640.40	19051.39	317.52
35	11190.80	18315.55	305.26	11003.00	18008.18	300.14	11278.80	18459.57	307.66	10933.80	17894.93	298.25	11620.40	19018.66	316.98	10818.60	17706.38	295.11
50	10853.20	17763.01	296.05	11255.00	18420.62	307.01	10998.80	18001.31	300.02	10007.20	16378.40	272.97	10008.80	16381.01	273.02	11249.80	18412.11	306.87
63	7882.60	12901.15	215.02	8895.00	14558.10	242.64	8055.40	13183.96	219.73	8331.60	13636.01	227.27	7935.20	12987.23	216.45	7991.00	13078.56	217.98
78	7049.00	11536.82	192.28	8724.20	14278.56	237.98	8435.20	13805.56	230.09	7022.80	11493.94	191.57	7102.20	11623.90	193.73	7705.20	12610.80	210.18
91	8046.40	13169.23	219.49	7826.80	12809.82	213.50	7623.20	12476.60	207.94	7587.20	12417.68	206.96	7200.80	11785.27	196.42	7813.40	12787.89	213.13
106	7577.40	12401.64	206.69	7784.80	12741.08	212.35	7936.20	12988.87	216.48	7656.20	12530.61	208.84	7710.40	12619.31	210.32	7660.00	12536.82	208.95

b) Calcite 120 & 60 resuspended in a pH 7.5 equilibrated solution, calculations CPM to Bq

	Calcite 120 Control			Calcite 120 Sample 1			Calcite 120 Sample 2			Calcite 60 Control			Calcite 60 Sample 1			Calcite 60 Sample 2		
Time (days)	cpm	dpm	Bq	cpm	dpm	Bq	cpm	dpm	Bq	cpm	dpm	Bq	cpm	dpm	Bq	cpm	dpm	Bq
0	14652.00	23980.36	399.67	12191.00	19952.54	332.54	14283.60	23377.41	389.62	13534.40	22151.23	369.19	13945.40	22823.90	380.40	14609.00	23909.98	398.50
1	12900.20	21113.26	351.89	14328.60	23451.06	390.85	14559.20	23828.48	397.14	12864.00	21054.01	350.90	12792.20	20936.50	348.94	13837.80	22647.79	377.46
2	12379.80	20261.54	337.69	11886.00	19453.36	324.22	13308.80	21782.00	363.03	14100.00	23076.92	384.62	11990.20	19623.90	327.06	13396.20	21925.04	365.42
3	13585.40	22234.70	370.58	13948.80	22829.46	380.49	14428.20	23614.08	393.57	14394.00	23558.10	392.64	14141.00	23144.03	385.73	14739.00	24122.75	402.05
4	13880.40	22717.51	378.63	14061.40	23013.75	383.56	12252.00	20052.37	334.21				13660.20	22357.12	372.62	13003.20	21281.83	354.70
6	14429.00	23615.38	393.59	14252.20	23326.02	388.77	14818.60	24253.03	404.22	12946.40	21188.87	353.15	12234.60	20023.90	333.73	14684.40	24033.39	400.56
10	13253.80	21691.98	361.53	13660.20	22357.12	372.62	13897.40	22745.34	379.09	13521.20	22129.62	368.83	13486.60	22073.00	367.88	13956.00	22841.24	380.69
15	13297.20	21763.01	362.72	12961.20	21213.09	353.55	13784.60	22560.72	376.01	12020.80	19673.98	327.90	13000.40	21277.25	354.62	13381.40	21900.82	365.01
22	12377.00	20256.96	337.62	12765.00	20891.98	348.20	12794.20	20939.77	349.00	12855.00	21039.28	350.65	12073.80	19760.72	329.35	12555.00	20548.28	342.47
29	10123.00	16567.92	276.13	9766.40	15984.29	266.40	11012.20	18023.24	300.39	11384.00	18631.75	310.53	12062.20	19741.73	329.03	11450.60	18740.75	312.35
35	9490.60	15532.90	258.88	11685.40	19125.04	318.75	11332.60	18547.63	309.13	11316.40	18521.11	308.69	11595.40	18977.74	316.30	11844.40	19385.27	323.09
50	10790.60	17660.56	294.34	10435.80	17079.87	284.66	10309.00	16872.34	281.21	11053.20	18090.34	301.51	10196.40	16688.05	278.13	11488.20	18802.29	313.37
63	8183.00	13392.80	223.21	8667.00	14184.94	236.42	8829.60	14451.06	240.85	8692.00	14225.86	237.10	8690.60	14223.57	237.06	8789.40	14385.27	239.75
78	8628.60	14122.09	235.37	8813.80	14425.20	240.42	8889.20	14548.61	242.48	7839.60	12830.77	213.85	7970.40	13044.84	217.41	8628.80	14122.42	235.37
91	6489.20	10620.62	177.01	5499.80	9001.31	150.02	7446.00	12186.58	203.11	7731.00	12653.03	210.88	7671.00	12554.83	209.25	7457.20	12204.91	203.42
106	7655.00	12528.64	208.81	7807.80	12778.72	212.98	7945.60	13004.26	216.74	7527.60	12320.13	205.34	7540.60	12341.41	205.69	6728.40	11012.11	183.54

Table.6 Calcite crystallinity based on Full Width Half Maximum

Calcite	Full Width Half Maximum
120	0.164
120-1	0.154
60	0.235
60-1	0.132
30	0.128
30-1	0.175

Table 7. Calcite resuspension in equilibrium: pH evolution

a) pH evolution of calcite 120 & 60 resuspended in initial equilibrium pH 8.4

Days	Calcite 120, pH 8.3			Calcite 60, pH 8.3		
	Blank	Sample 1	Sample 2	Blank	Sample 1	Sample 2
Day 35	8.1	8.17	8.17	7.92	8.06	8.06
Day 50	7.31	8.1	8.11	7.83	8.03	7.94
Day 63	8.14	8.04	8.06	7.87	8.06	7.97
Day 78	7.93	7.96	7.95	7.67	7.89	7.81
Day 91	7.96	8.01	8.13	7.75	7.92	7.94
Day 106	7.93	8.02	8.01	7.73	7.89	7.88

b) pH evolution of calcite 120 & 60 resuspended in initial equilibrium pH 7.5

Days	Calcite 120, pH 7.5			Calcite 60, pH 7.5		
	Blank	Sample 1	Sample 2	Blank	Sample 1	Sample 2
Day 35	7.32	7.37	7.35	7.33	7.34	7.44
Day 50	7.27	7.29	7.37	7.26	7.39	7.39
Day 63	7.21	7.33	7.35	7.19	7.39	7.38
Day 78	7.06	7.19	7.21	7.12	7.25	7.22
Day 91	7.18	7.26	7.28	7.13	7.32	7.31
Day 106	7.17	7.24	7.27	7.08	7.31	7.29

Appendix B: Figures

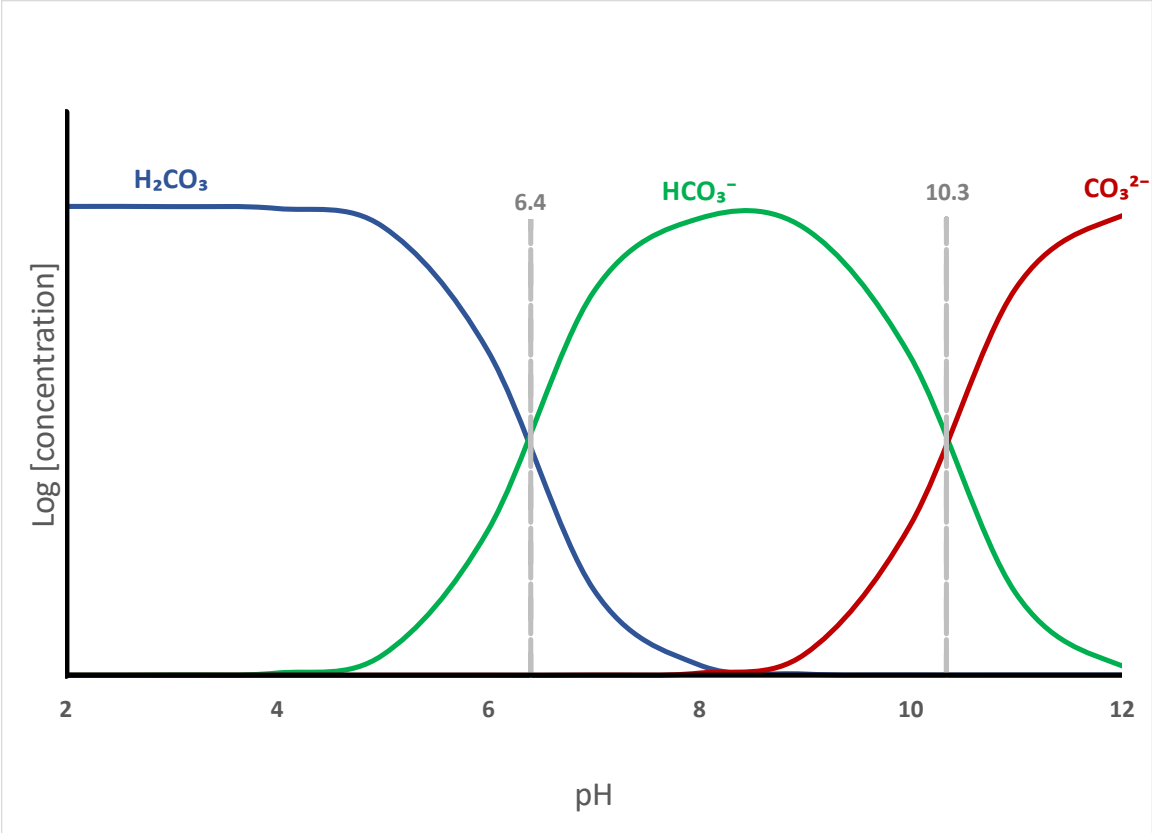

Fig.1 Carbonate Log C pH diagram: When pH<6.35, H_2CO_3 is the dominant species. When 6.35<pH<10.33, HCO_3^- is the dominant species in solution. When pH<10.33, CO_3^{2-} dominates in solution.

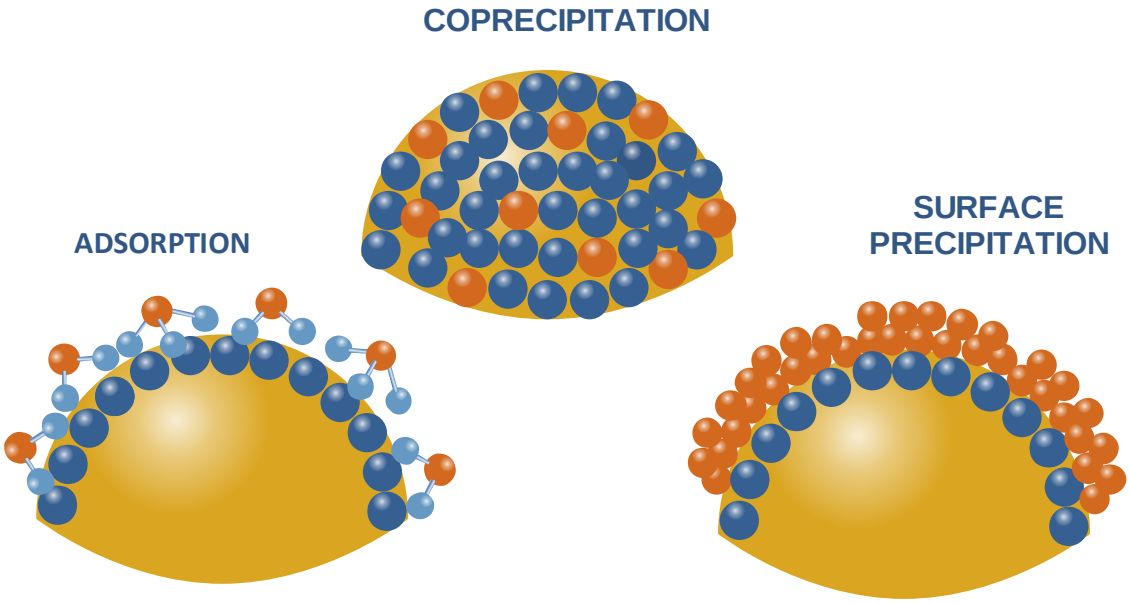

Fig.2 Sorption. Adsorption is a surface bond between element and mineral with typically a layer of hydration between the bond. During coprecipitation an element is incorporated into bulk of mineral lattice. Surface precipitation is the precipitation of a second mineral upon surface of initial mineral.

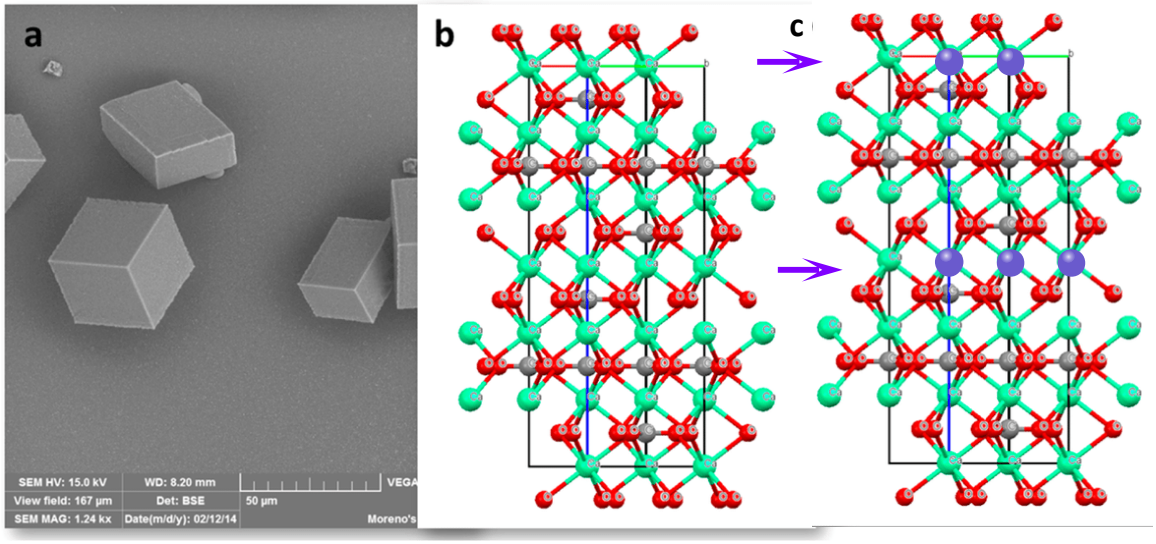

Fig.3 Recrystallization. a) Scanning electron microscopy (SEM) image of calcite single crystal (from Moreno A., Ruiz-Arellano R.R, 2014). b) $CaCO_3$ lattice in 3D space (from Moreno A., Ruiz-Arellano R.R, 2014). c) The exchange of Ca^{2+} atoms at the surface and bulk calcite lattice layers.

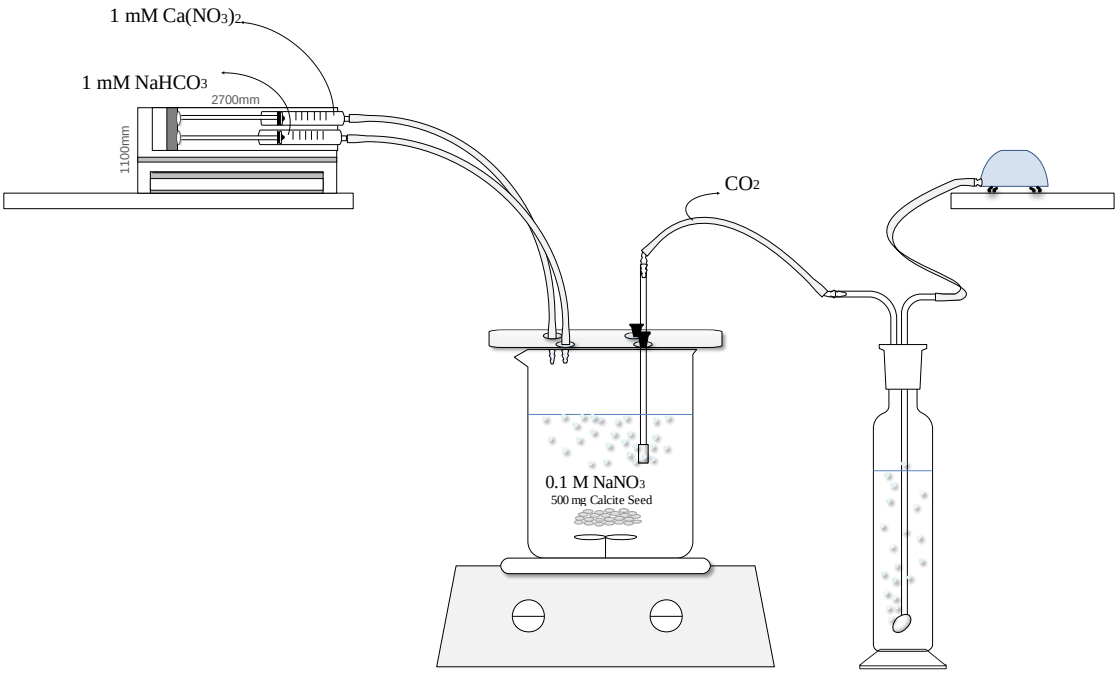

Fig.4 Calcite experimental growth set up via the constant addition method. Calcite seed is added for nucleation in a sodium nitrate background solution, while $CO_{2(g)}$ is added from a tank and calcium nitrate and sodium bicarbonate are pumped in with a syringe pump.

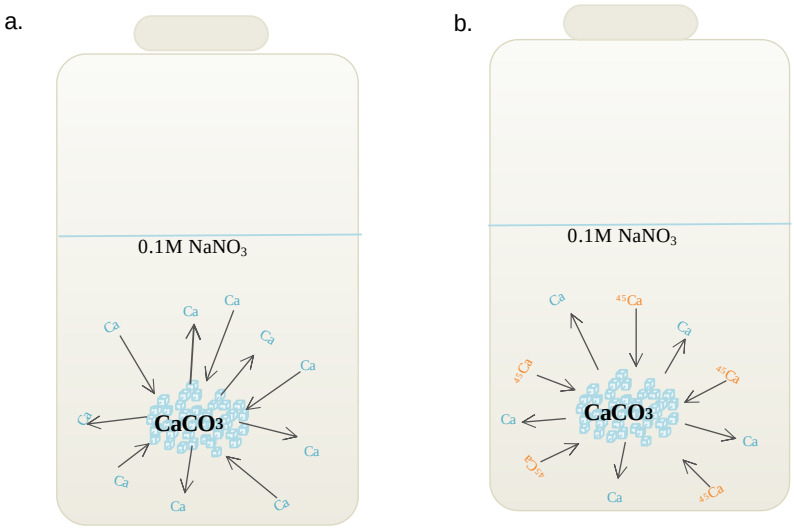

Fig.5 Calcite exchange: a) Calcite resuspended in solution with equilibrated concentration of Ca. Calcite in this solution has the potential to exchange its Ca ions with ^{40}Ca stable isotope. b) Calcite resuspended in solution with equilibrated concentration^{45}Ca. Calcite in this solution has the potential to exchange its Ca ions with ^{45}Ca radioactive isotope

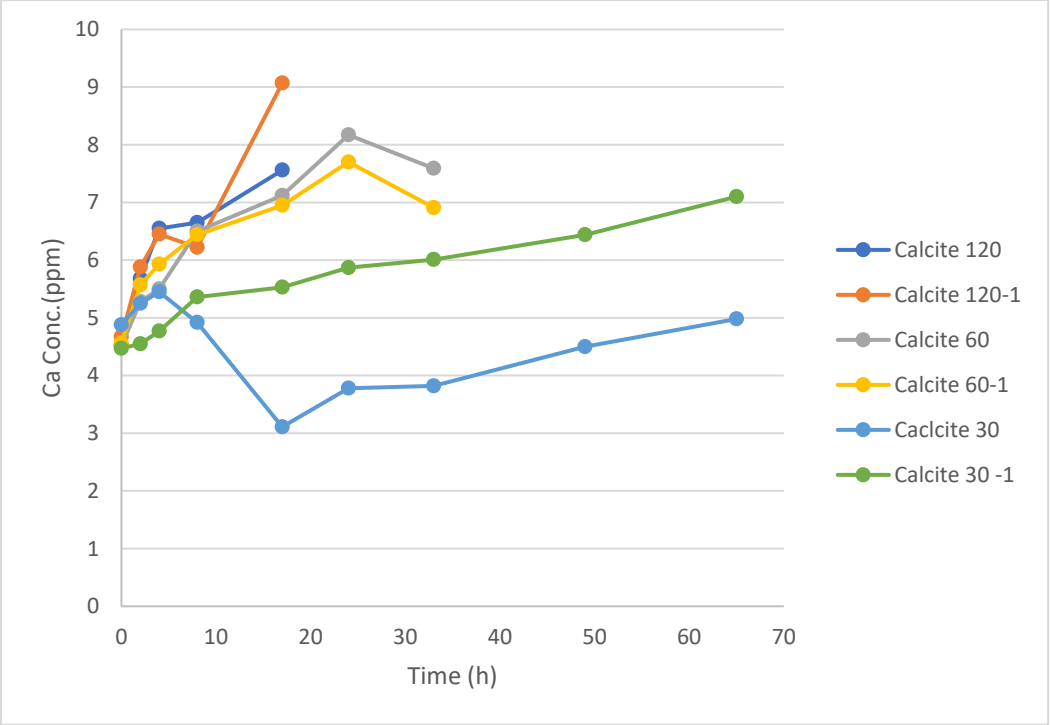

Fig.6 Calcite growth Ca concentrations in parts per million. Calcite 120 and its duplicate120-1 have the shortest growth time and reach higher concentrations of calcium as a result of fast pump rate which incorporates less calcium into the solid. Calcite 60 and its duplicate 60-1 increase in concentration over time and show intermediate results. Calcite 30 and its duplicate 30-1 have the shortest growth time with a slower pump rate there is less calcium present in solution, relative to the other calcites, as more is incorporated into the solid. All solutions have increasing Ca concentrations due to the constant addition of calcium nitrate.

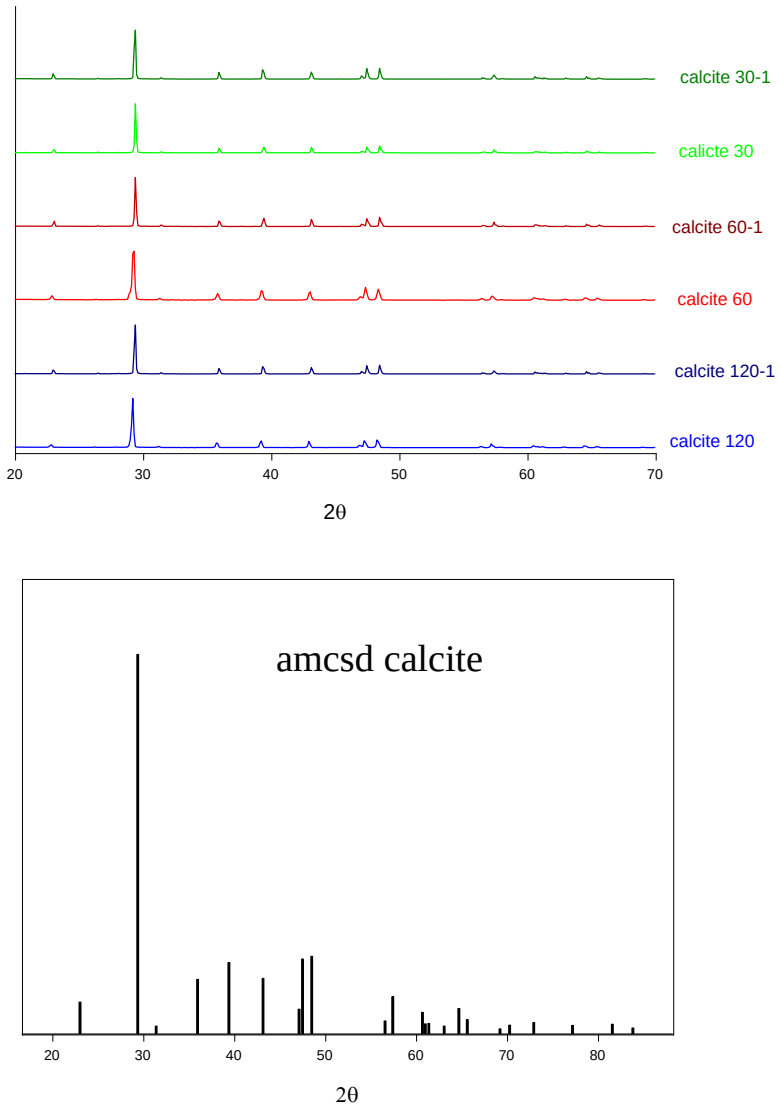

Fig.7 XRD of calcite 120, 60, 30 and their duplicates. Amcsd values of calcite are in the bottom graph. All samples demonstrate characteristic calcite diffraction peak at the 2θ = 29.4º value.

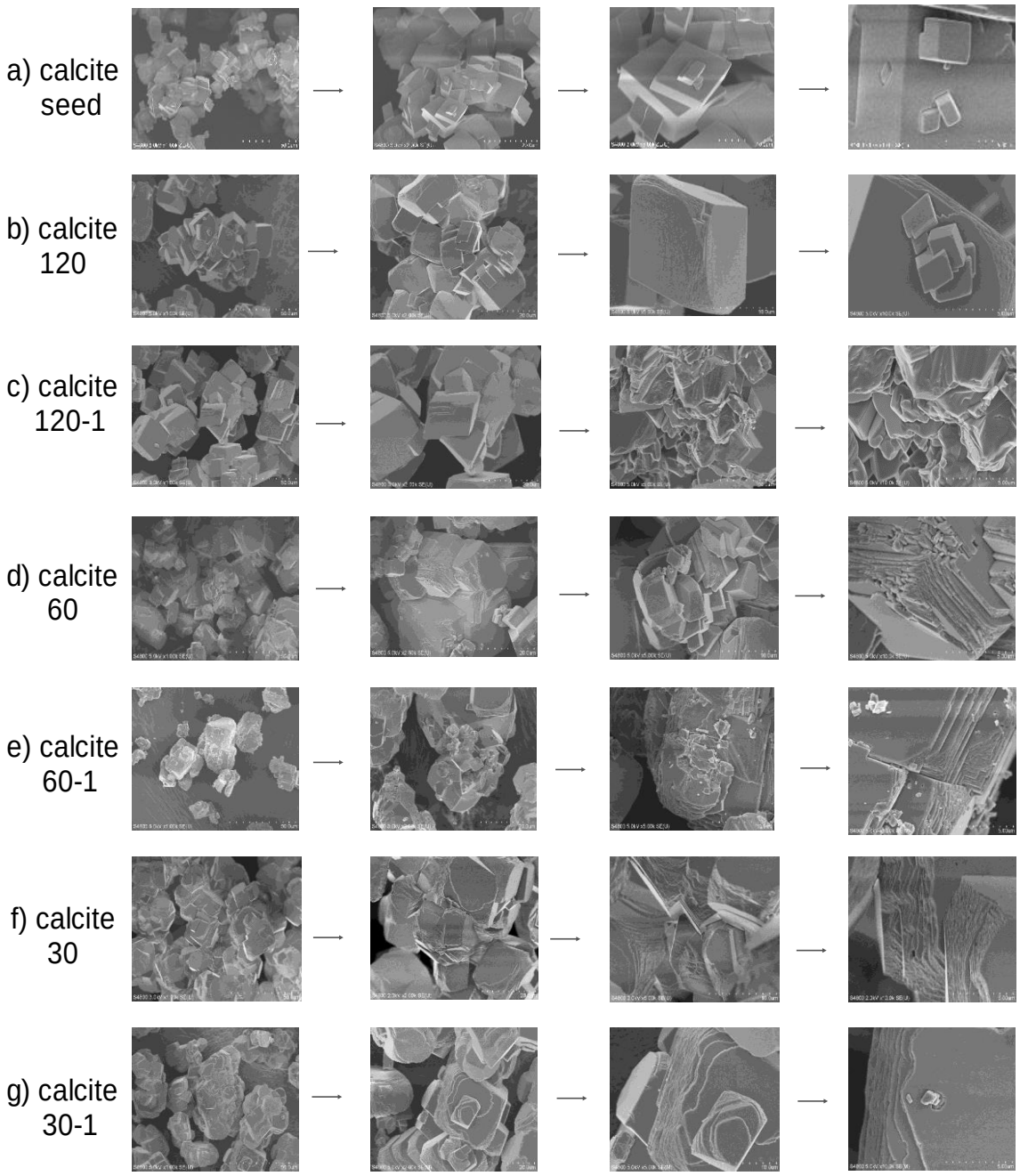

Fig.8 SEM micrograph of a) the calcite seed used b & c) calcite 120, its duplicate 120-1, d & e) 60, its duplicate 60-1, and f & g) calcite30 and its duplicate30-1. All calcite grown at syringe pump 120 µL/min has a structure similar to the calcite seed with the exception of few overgrowths. Calcite grown at syringe pump 60 µL/min begin to show significant overgrowth of layers. Calcite 30 has the most overgrowths, however, is still characteristic of the typical calcite rhombohedron structure.

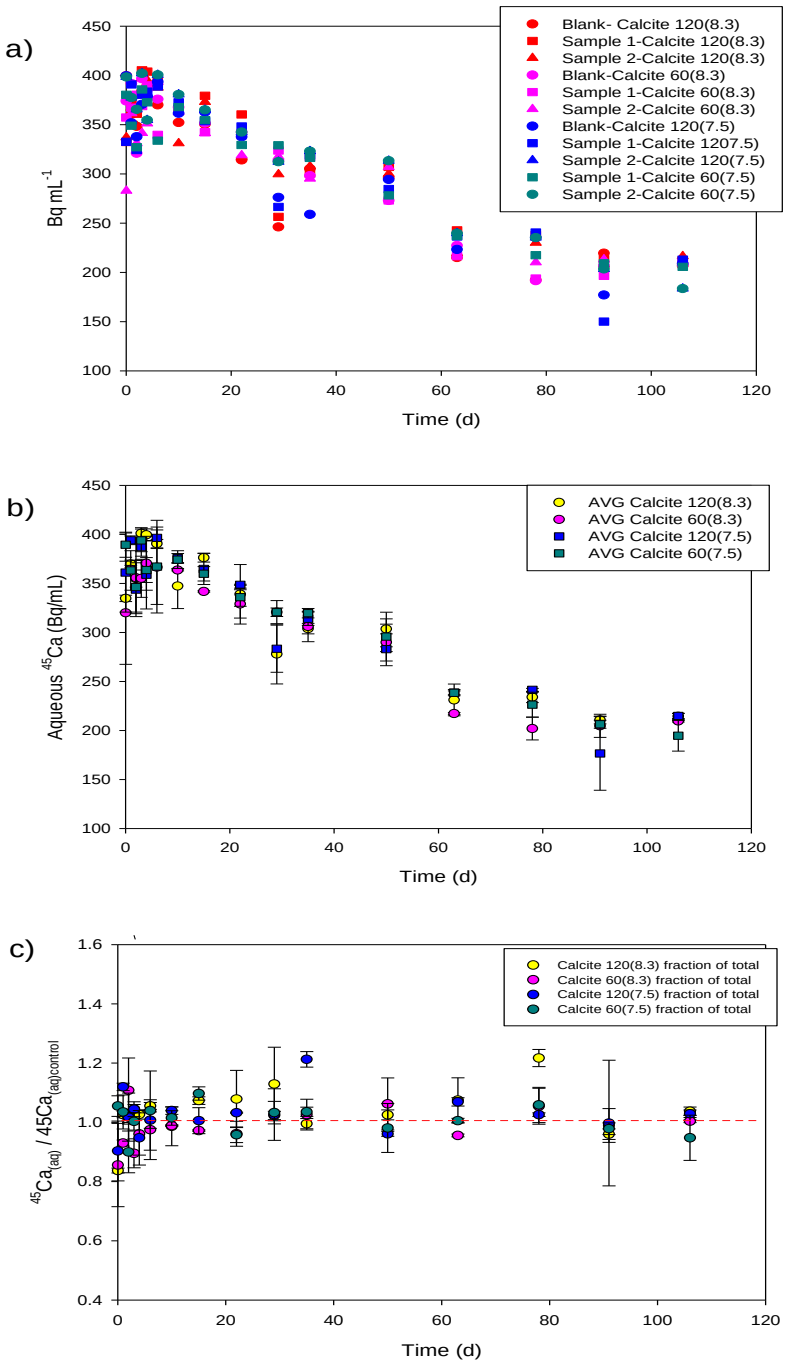

Fig.9 All ^{45}Ca radiotracer resuspension experiments. a) Plotting of the raw data (of all calcite samples for both pH 8.3 and pH 7.5) from the scintillation counter, the concentration of radioisotope in Becquerels is in the y-axis, over time in the x-axis. There is a steady decrease in the ^{45}Ca radioisotope that is in solution and is attributed to the isotopes natural decay. b) The average ^{45}Ca activity over time in Bq/mL and .c) expressed as the fraction of the total aqueous ^{45}Ca added.

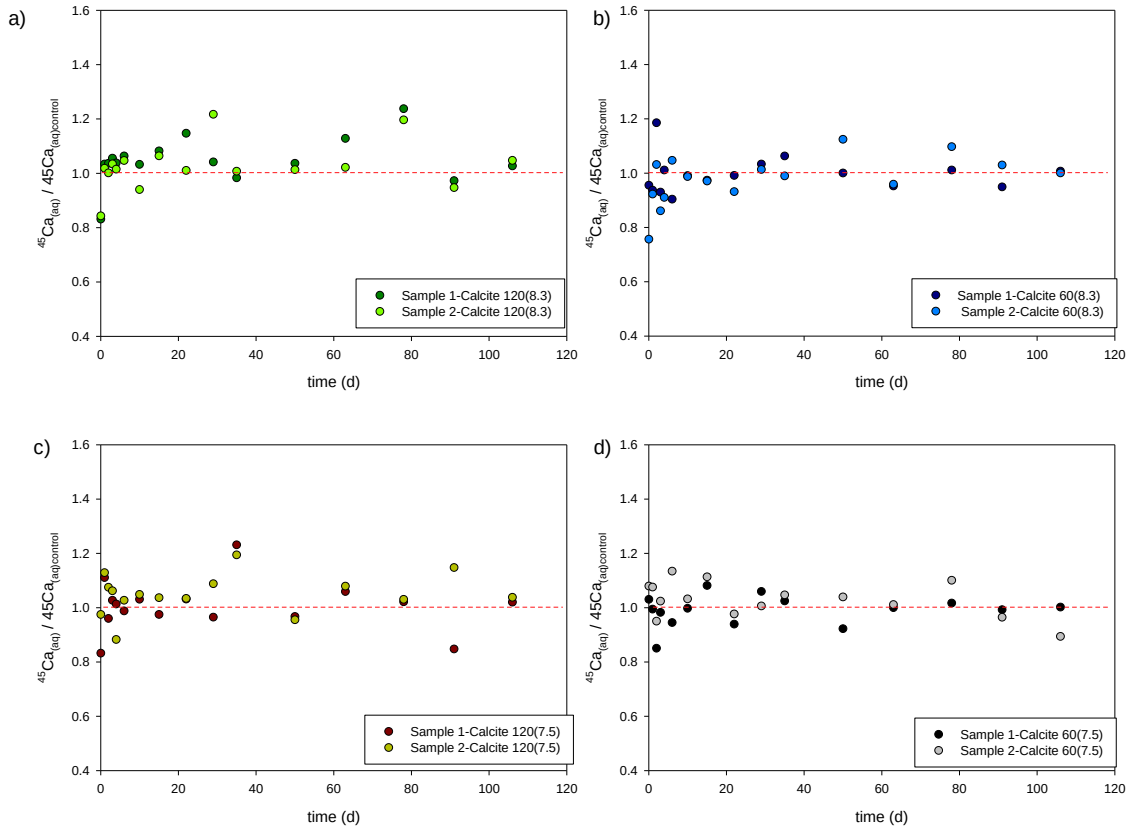

Fig.10 ^{45}Ca Radiotracer resuspension experiments for pH 8.3 and pH 7.5. Figure 10a) shows that calcite 120 grown at a faster rate and b) calcite 60 grown at a slower rate, both exhibit concentrations that run parallel to the red 1:1 solid liquid ratio over time for the variable pH 8.3. Figure 10c) and d) also demonstrate concentrations along the red 1:1 ratio line, with equal concentrations in solid and liquid species under pH 7.5. All batches demonstrate dynamic equilibrium.

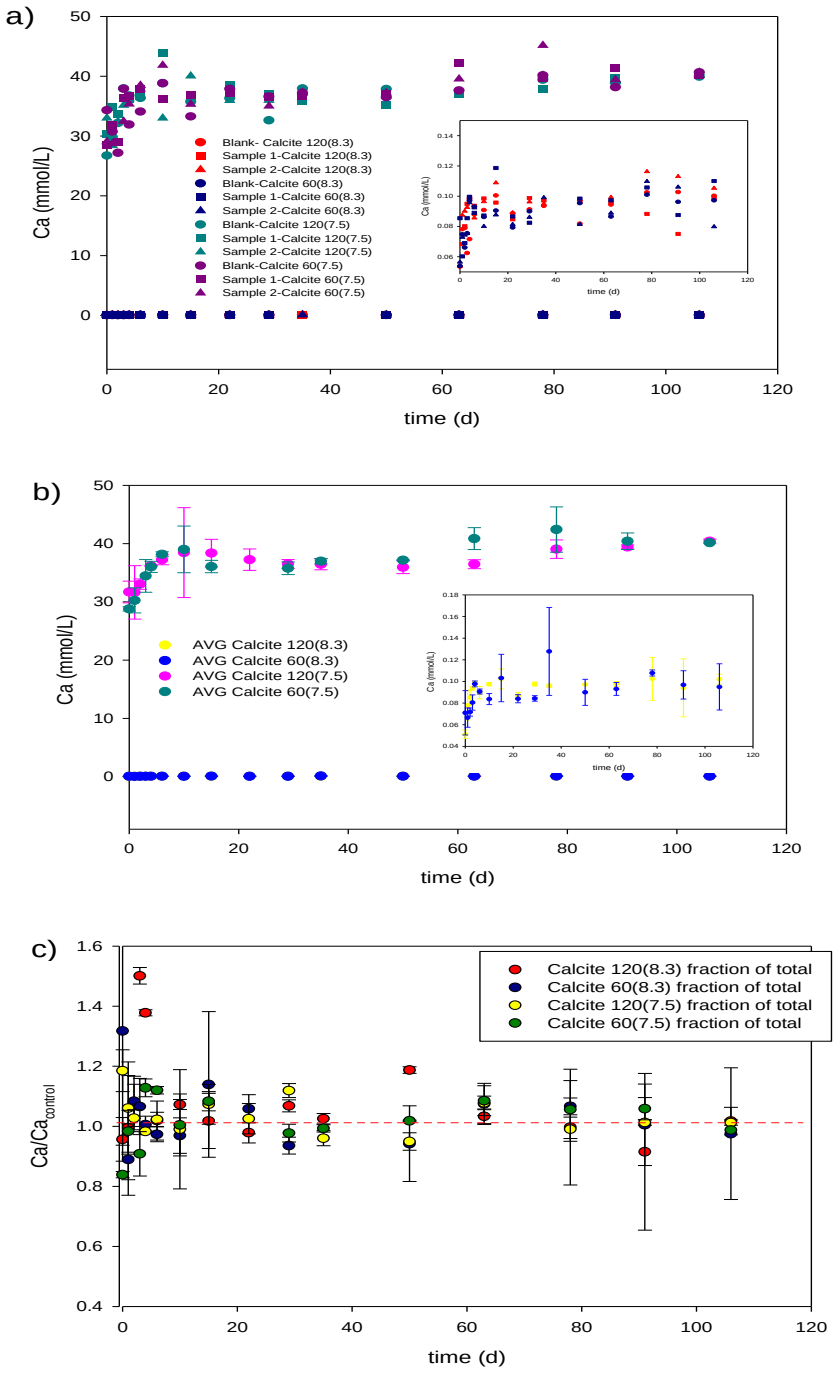

Fig.11 All ^{40}Ca stable isotope resuspension experiments. a) Sample of all calcite from resuspension experiments of pH 8.3 and pH 7.5 are plotted in mmol/L over time. For pH 8.3 calcium concentrations increase for approximately 18 days before stabilizing. b) the average ^{40}Ca concentration over time, this image also demonstrates stabilization after 18 days. c) is expressed in the fraction of total aqueous ^{40}Ca present. The red dotted line indicates equilibrium.

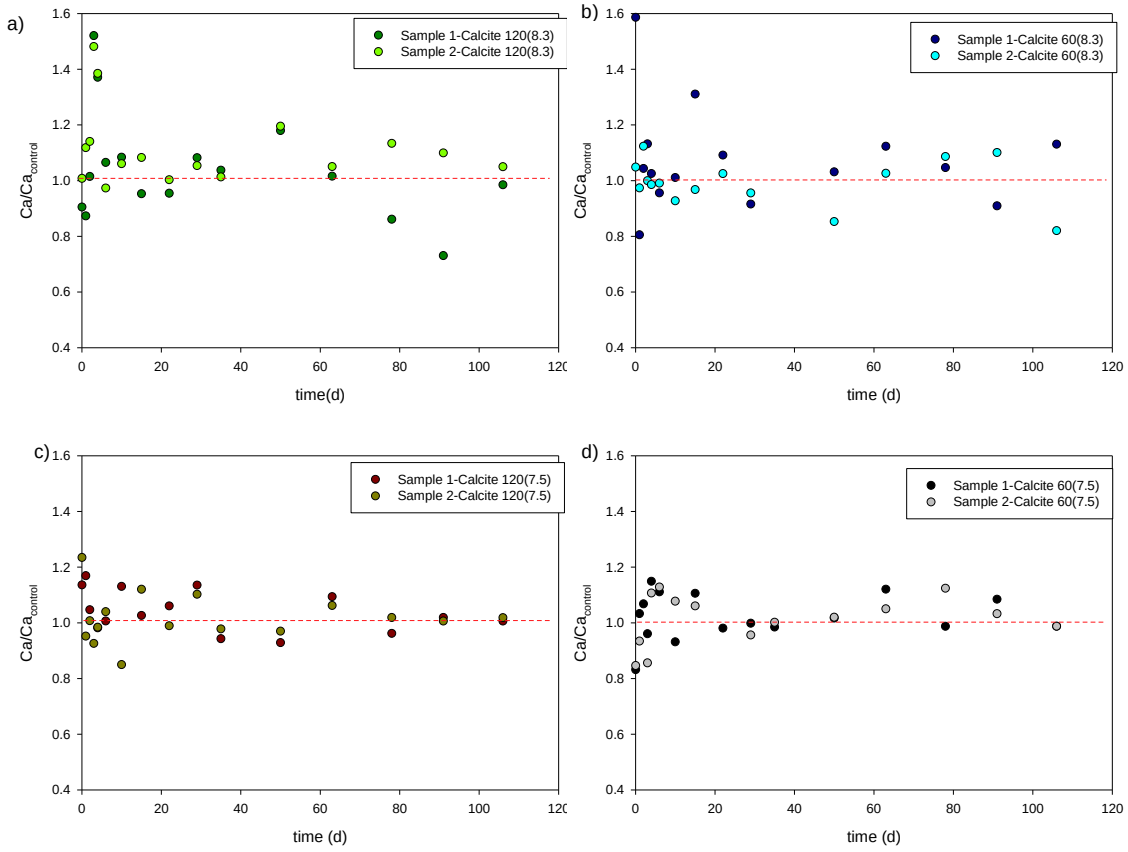

Fig.12 ^{40}Ca stable isotope resuspension experiments for pH 8.3 and 7.5. Fig 12a-d are a more focused view of Fig.11. In 12a and 12b there is equilibrium occurring in experiments under pH 8.3, demonstrated by the concentration of plots around the red dotted line of the 1:1 ratio. Fig 12c and 12d also shows the scatter along the equilibrium line for experiment and their duplicates under pH 7.5.

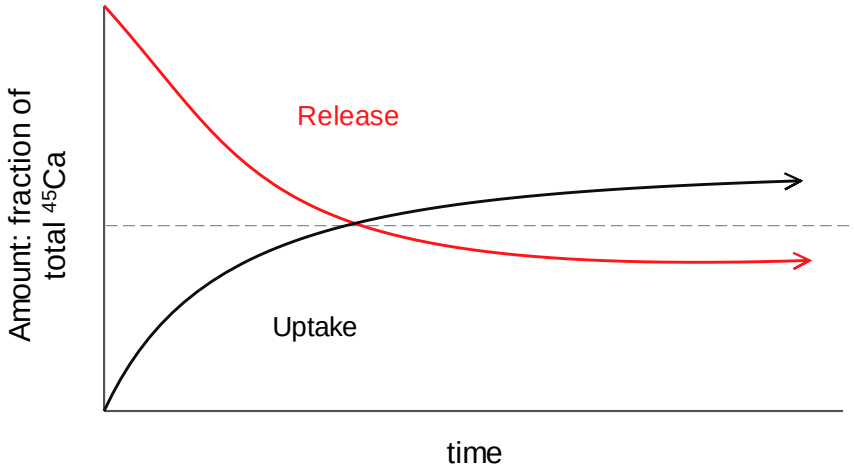

Fig.13 Logarithmic equilibration graph depicts concentration in terms of fraction of total ^{45}Ca over time. Equilibrium of the system is reached when the reactants(release) and products(uptake) are no longer changing and their concentrations stabilize.

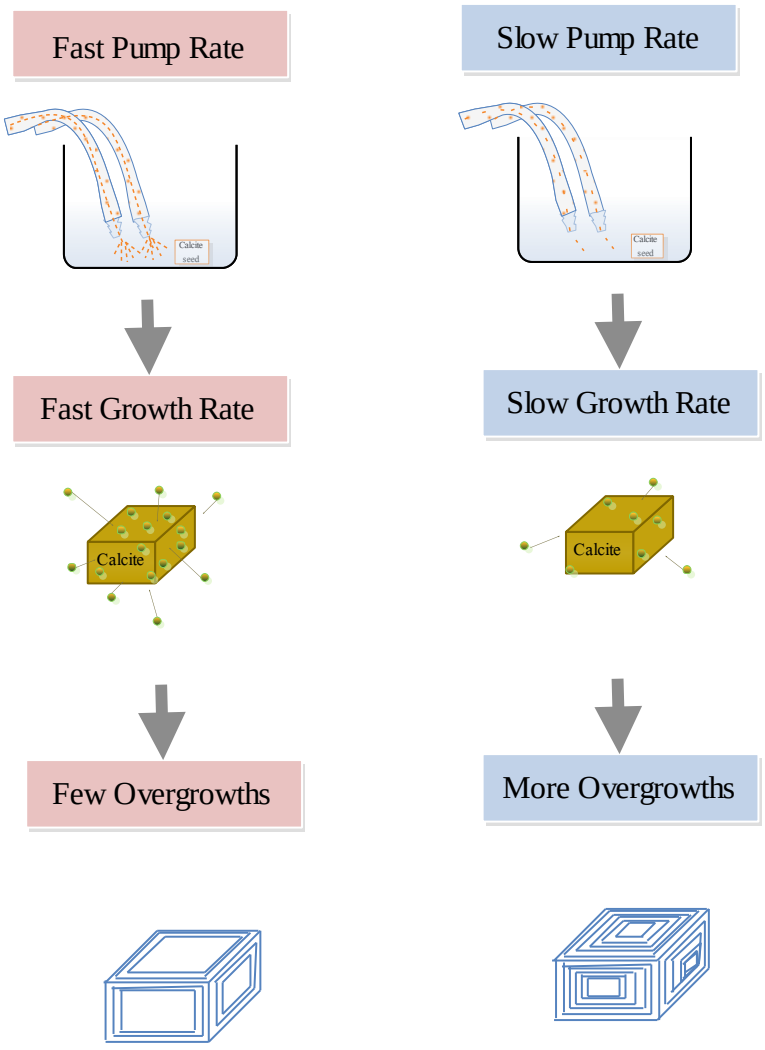

Fig 14 Calcite overgrowths as a result of growth rate and syringe pump rate. A fast syringe pump rate, such as 120 µL/min, results in a faster growth rate and fewer overgrowths. Slower pump rates, such as 30 µL/min, results in slower growth rate and as a result there is more time available for the mineral to increase overgrowth layers.

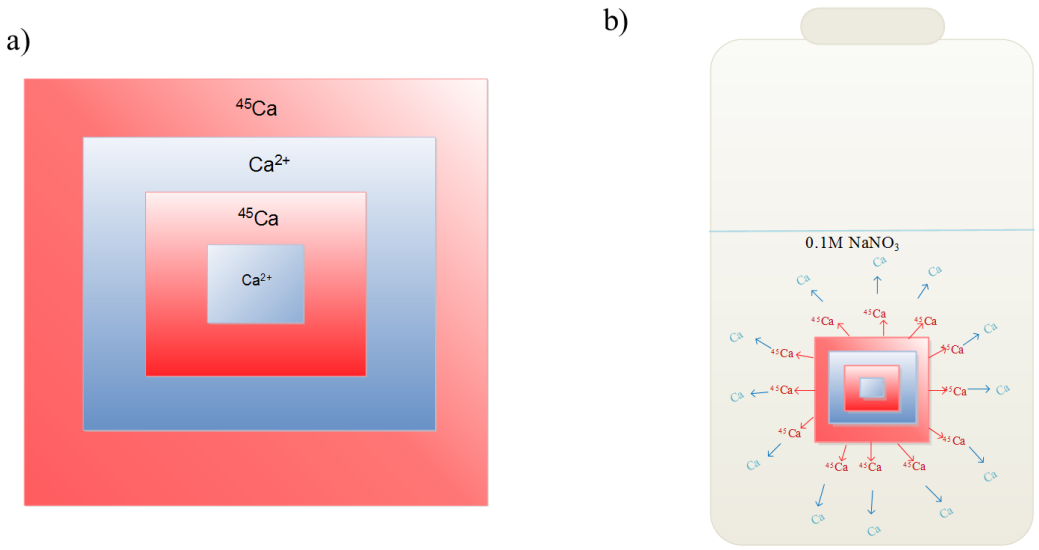

Fig. 15 a) Calcite growth with alternating layers of ^{40}Ca and ^{45}Ca isotope 15b) Grown calcite with alternating layers of ^{40}Ca and ^{45}Ca isotope is resuspended and allowed to react for exchange/release. When exchange is to occur, the outer layers are thought to react first and over time, the inner mineral layers would also react if there is sufficient driving force. Once the ^{45}Ca radioisotope within the mineral is released into solution, the experiment is able to detect recrystallization.